UNLV | UNIVERSITY LIBRARIES

1-1-2008

Monitoring and modeling the performance of a solar powered hydrogen filling station

Mark R Campbell
University of Nevada, Las Vegas

Follow this and additional works at: https://digitalscholarship.unlv.edu/rtds

MONITORING AND MODELING THE PERFORMANCE

OF A SOLAR POWERED HYDROGEN

FILLING STATION

by

Mark R. Campbell

Bachelor of Science, Mechanical Engineering
University of Pittsburgh
2004

A thesis submitted in partial fulfillment
of the requirements for the

Master of Science Degree in Mechanical Engineering
Department of Mechanical Engineering
Howard R. Hughes College of Engineering

Graduate College
University of Nevada Las Vegas
August 2008

UMI Number: 1460460

INFORMATION TO USERS

The quality of this reproduction is dependent upon the quality of the copy submitted. Broken or indistinct print, colored or poor quality illustrations and photographs, print bleed-through, substandard margins, and improper alignment can adversely affect reproduction.

In the unlikely event that the author did not send a complete manuscript and there are missing pages, these will be noted. Also, if unauthorized copyright material had to be removed, a note will indicate the deletion.

UNLV

Thesis Approval

The Graduate College

University of Nevada, Las Vegas

July 9 ,20 08

The Thesis prepared by

Mark R Campbell

Entitled

Monitoring and Modeling the Performance of a Solar Powered

Hydrogen Filling Station

is approved in partial fulfillment of the requirements for the degree of

Master of Science in Mechanical Engineering

Examination Committee Chair

Dean of the Graduate College

Examination Committee Member

Examination Committee Member

Graduate College Faculty Representative

ABSTRACT

**Monitoring and Modeling the Performance of a Solar Powered
Hydrogen Filling Station**

By

Mark R. Campbell

Dr. Robert F. Boehm, Examination Committee Chair
Distinguished Professor, Mechanical Engineering
University of Nevada Las Vegas

A hydrogen filling station (HFS) has been constructed in Las Vegas to demonstrate

how solar energy can be used to generate and store hydrogen as an energy carrier for

transportation. This thesis presents a description of the station and the data acquisition

system used to monitor its performance. Energy consumption by the hydrogen generation

and storage equipment and energy production from a solar photovoltaic (PV) array were

measured, and based on the characteristics of the different system components, a

computer model was created to predict the amount of hydrogen that could be produced

from the solar array. The hydrogen produced at the station is used by several converted

vehicles, and the model is able to simulate the operation of the station based on a given

level of vehicle usage.

TABLE OF CONTENTS

LIST OF FIGURES

LIST OF TABLES

NOMENCLATURE

Variable/Abbreviation	Description
a	Modified ideality factor
a, b	Parameters used to calculate R_b
a_c, b_c	Empirical constants for cell temperature calculation
A_{pv}	Area of PV module (m^2)
AC	Alternating Current
CER	Center for Energy Research
CCS	Continental Control Systems
CSI	Campbell Scientific Incorporated
DAS	Data Acquisition System
DC	Direct Current
DOE	Department of Energy
E_{PV}	Energy output from PV panels
F_1, F_2	Brightness coefficients used for diffuse radiation calculation ($I_{d,T}$)
GHG	Greenhouse Gases
HFS	Hydrogen Filling Station
HHV	Higher Heating Value
I_{NOCT}	Instantaneous solar irradiation at standard rated conditions (1000 W/m^2)
I	Global horizontal radiation (W/m^2)
I_b	Beam radiation on a horizontal surface (W/m^2)
I_d	Total diffuse radiation on horizontal surface (W/m^2)
$I_{d,T}$	Total diffuse radiation on tracking surface (W/m^2)
I_T	Instantaneous total solar irradiation on PV (W/m^2)
I_L	Light Current (A)
I_{mp}	Current at Maximum Power Point (A)
I_O	Diode reverse saturation Current (A)
I_{pv}	Current of PV panel (A)
I_{sc}	Short Circuit Current (A)
ICE	Internal Combustion Engine
k	Boltzmann's constant (1.381x10^{-23} J/K)
LVVWD	Las Vegas Valley Water District
n	Ideality factor used to calculate a
N_{PV}	Number of cells in series
NEMA	National Electrical Manufacturers' Assoc.
NPC	Nevada Power Company
PDC	Pressure Dynamic Consultants
PEM	Polymer Electrolyte Membrane
PV	Photovoltaic

q	Electronic charge (1.609×10^{-19} A-s)
R_b	Ratio of beam radiation on a tilted surface to that on a horizontal surface
R_s	Series resistance (Ω)
R_{sh}	Shunt resistance (Ω)
RTDM	Real-Time Data Monitoring
T_a	Ambient temperature (K)
$T_{m,pv}$	Back surface temperature of PV module (K)
T_{pv}	Cell temperature of PV (K)
U_{mp}	Voltage at Maximum Power Point (V)
U_{oc}	Open-circuit voltage (V)
U_{pv}	Voltage of PV cells (V)
UNLV	University of Nevada at Las Vegas
VDC	Volts, Direct Current
V_w	Wind Speed (m/s)

Greek Symbols

β	Surface slope of solar tracker
$\beta_o{}'$	Parameter used to find β, surface slope
β'	Slope of the solar tracker's axis
γ	Surface azimuth angle
γ'	Azimuth angle of tracking axis
$\eta_{c,pv}$	Module efficiency to convert incident solar irradiation to electrical energy
θ	Angle of Incidence
θ_z	Zenith Angle
μ_{oc}	Open-circuit Temperature Coefficient
μ_{sc}	Short-circuit Temperature Coefficient
ρ_g	Ground Reflectance
σ_β	Parameter used to find β, surface slope

ACKNOWLEDGEMENTS

I would like to thank Dr. Robert Boehm for giving me the opportunity to be a part of the Center for Energy Research. The guidance and flexibility he has given me during my time here has allowed me to learn and grow as a researcher and ambassador for renewable energy. Thank you to Rick Hurt, who contributed many hours answering questions, explaining different systems, and teaching me skills that I will be able to carry into the future. His work related to this project is the reason I was able to carry out the research contained in this thesis. Also, I would like to thank Sachin Deshmukh for the modeling expertise he shared while we worked together on the theoretical portion of this research. Additionally, I would like to thank all of the students and staff at the Center for Energy Research, who have kept me on track and been great companions for the past two years. Of course, without the support and strength of my family, I would not be in the position I am in today.

Thank you to the Department of Energy, who provided the funding for this project. Also, thank you to the Las Vegas Valley Water District (LVVWD) and Proton Energy Systems for their participation and assistance in the operation and maintenance of the hydrogen filling station.

CHAPTER 1

INTRODUCTION

A hydrogen filling station (HFS) has been installed in Las Vegas to demonstrate how solar energy can be used to generate fuel for transportation. The hydrogen is generated by a Proton Exchange Membrane (PEM) electrolyzer, and stored on site for use in hydrogen fueled vehicles converted as a part of this project. Power for the equipment is provided by a solar photovoltaic (PV) array. A data acquisition system (DAS) was installed at the station to monitor the performance of the equipment and also weather conditions. Additionally, a computer model was created to simulate the operation of the station. The model is a way to predict the way the HFS uses and produces power, based on the climate and a specified amount of hydrogen usage. The experimental and theoretical results from this research will describe the performance of the HFS, which can be used to identify areas for improvement and ongoing research within the alternative fuel arena.

Project Background

In 2003, with funding from the Department of Energy, the UNLV Research Foundation formed a research partnership between the UNLV Center for Energy Research (CER), the Las Vegas Valley Water District (LVVWD), Kell's Automotive and Marine (KAM) and Proton Energy Systems, with the purpose of designing and installing a HFS. Each of the project partners devoted time and energy to construct the station, and had their own objectives for the project. The LVVWD has a goal to use only alternatively

1

fueled vehicles, including hydrogen powered vehicles, and they donated several of them for conversion, as well as their own land as the location for the HFS. Proton Energy Systems designed and installed the electrolyzers (hydrogen generation equipment), and uses the station as a place to observe the performance and reliability of their systems. The UNLV CER's responsibility is to monitor the performance of each system at the HFS as well as maintain it, in the case of small errors or regular maintenance procedures.

Hydrogen as a Fuel for Transportation

Hydrogen has the potential to be an important fuel in the future because of its ability to be produced, stored and used at one location, for a variety of applications where fossil fuels are currently used. The U.S. Department of Energy (DOE) reports that more than one-half of the petroleum used in the United States is imported, and that fraction is expected to increase to 68% by 2025 [1]. Two-thirds of that imported oil is used by the U.S. transportation sector [2]. In 2003, the greenhouse gases (GHG) emitted from the transportation sector accounted for 27% of the total GHG emissions in the United States, representing the largest percentage increase of any economic sector over the previous 13 year period [3].

Using hydrogen as a fuel for transportation has the potential to solve these issues simultaneously. The National Academies' National Research Council has issued a report stating, "A transition to hydrogen as a major fuel in the next 50 years could fundamentally transform the U.S. energy system, creating opportunities to increase energy security through the use of a variety of domestic energy sources for hydrogen production while reducing environmental impacts, including atmospheric CO_2 emissions and criteria pollutants." [4]. Hydrogen can be used as a fuel for a vehicle by burning it in

2

an internal combustion engine (ICE), or by mixing it with air inside a fuel cell to generate electricity. In the case of an ICE, the hydrogen is burned inside the engine cylinder in the same manner as gasoline, but the exhaust products are water and traces of nitrogen oxides [5]. A fuel cell driven vehicle relies on the fact that energy is released when hydrogen and the oxygen in air are reacted to form water. It has been shown that hydrogen fuel cells can be over 2.5 times more efficient than gasoline engines, and the exhaust product is only water [6].

Hydrogen is an energy carrier, meaning that it can deliver energy, but requires some form of energy to be separated from the other molecules in its various compounds (i.e. CH_4, H_2O). Hydrogen gas can be produced from fossil fuels via a process called reformation, but its greatest attribute is that it can be produced from water. The process shown in Figure 1, called electrolysis, involves introducing an electric current through water in order to create a chemical reaction that results in hydrogen and oxygen gas production. This process is the same reaction that takes place in a fuel cell, but reversed. In this case a source of electricity is required, and although hydrogen is a very clean fuel, there would still be GHG emissions produced by traditional electric power plants if they were used as that source. Conversely, producing hydrogen from renewable energy sources provides a sustainable way to power hydrogen vehicles in the future [7].
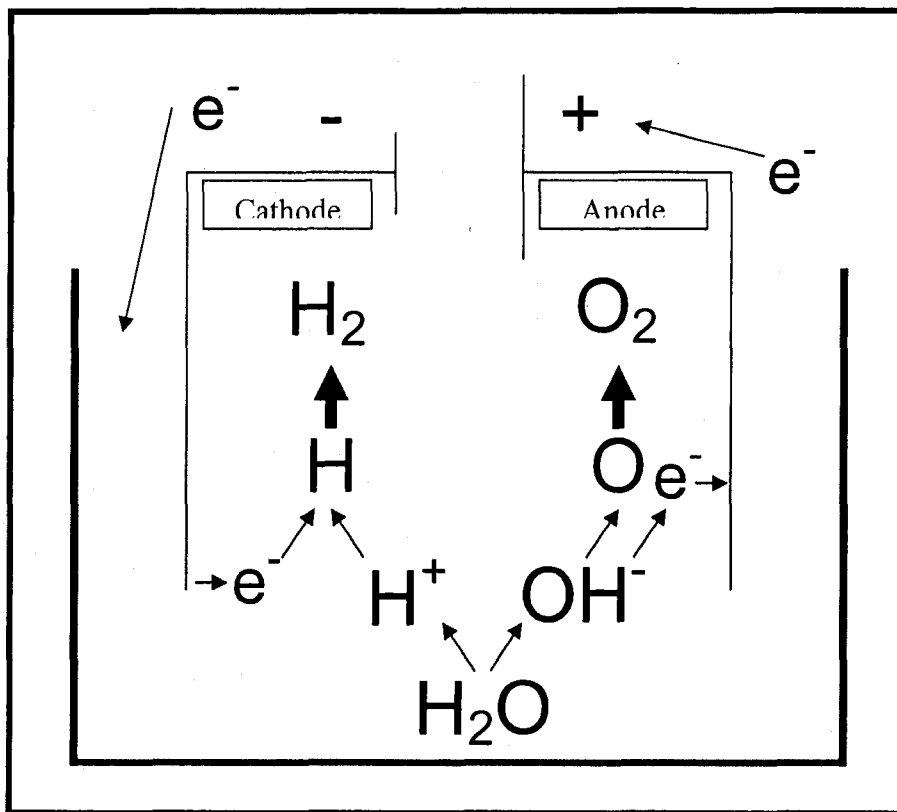
Figure 1. This figure illustrates the process of electrolysis, the splitting of water.

The idea of using hydrogen for transportation is not without its share of issues that

must be resolved through research and development before it becomes a large-scale

reality. Since hydrogen gas has a low volumetric energy density, it must be compressed

and stored in robust tanks in order to provide enough fuel for a vehicle to drive a

reasonable distance. Compression of the gas requires additional energy, and adding heavy

high pressure tanks to a vehicle increases its mass and requires a more robust material to

be used. Additionally, since hydrogen has a very high flammability range, significant

care must be taken with respect to designing vehicle's fuel system so that safety for all is

ensured. The result of these issues is that currently, creating and supporting the hydrogen

vehicle industry is expensive. Because of this great expense, there is a lack of

infrastructure to provide reliable fuel for hydrogen vehicles. Hydrogen filling stations like

the one described in this thesis can be used to address these issues by demonstrating the operation and performance that can be expected, and revealing the areas in which improvement is necessary.

Purpose of Study

The promise of hydrogen as a fuel for transportation is appealing enough for research projects addressing all of the issues involved with its implementation to be investigated. The objectives of the research included in this thesis are to: 1) Show how a solar powered hydrogen production and storage system performs with respect to energy input and hydrogen output; 2) Describe the performance of such a station, in terms of the quantity of hydrogen it can output and the manner in which it operates during regular hydrogen usage; 3) Create a computer model that can simulate the station's operation and be applied to different climates and hydrogen demand scenarios.

Literature Review

The following is a review of relevant publications that have been used for guidance and comparison of the HFS project's design, performance, and theoretical model. The available literature includes data relating electrolysis and renewable energy, both via experimental data and theoretical models. Additionally, several publications describing how to model the output from the solar photovoltaic (PV) array were used. Information relating to the conversion and performance of several hydrogen vehicles was also obtained from the literature.

Renewable energy sources, including solar energy, provide an excellent source for the electricity required to perform electrolysis, because they produce no emissions and require little maintenance during operation [8]. Several authors have published studies to

examining how different renewable energy technologies can be used to power the electrolysis process. Nowotny et al. [5] provide a table summarizing the advantages and disadvantages of many different types of renewable energy technologies that could be used to produce hydrogen including solar PV, wind, geothermal, tidal, biomass, and photoelectrolytic (PE) solar to hydrogen. Ivy et al. [8] have reported summaries of renewable energy resources and energy requirements of producing hydrogen at fueling stations. The assumptions made in the paper include a solar PV efficiency of 10%, and a set value for the capacity factor of wind turbines based on the class of wind speed available. Additionally, it is assumed that an electrolyzer requires 53 kWh to produce one kilogram of hydrogen, which is basically stating that the electrolyzer is 75% efficient, since the higher heating value (HHV) of hydrogen is 39 kWh/kg. The analysis resulted in a conclusion that a combination of solar PV and wind power could be used to produce 8.7 times the year 2000 gasoline consumption in the United States, not including the energy required for the compression or delivery of hydrogen.

Conibeer and Richards provide an overview of hydrogen production and storage using solar PV for electrolysis, and also direct PE generation of hydrogen [9]. With assumed values for the electrolyzer efficiency and solar PV efficiency of 65% and 13.5%, respectively, the PV electrolyzer system had an efficiency of 8.8%, based on the HHV of hydrogen. The results for PE efficiency were based on previous research to be around 5%. The conclusion was that currently, solar PV as a power source for electrolysis is the more appropriate technology of the two.

Barbir [10] provides a description of the electrolysis process, as well as a review of several different solar PV arrangements that could be used to generate hydrogen. The

possibilities of having a grid-connected or grid-independent system, with or without on-site storage, are also discussed in this paper. In particular, the application described in this thesis, a grid-connected solar PV to PEM (Proton Exchange Membrane) electrolysis system, is described. A PEM electrolyzer has a polymer membrane and porous electrodes, and the materials used are metallic, typically platinum or platinum alloys. Figure 2 shows how the PEM electrolysis process works. When a direct current (DC) voltage is applied, water is split into oxygen, protons, and electrons on the anode, the protons pass through a polymer electrolyte membrane, and combine with electrons at the cathode to form hydrogen. From Barbir's work, it was noted that increasing hydrogen output pressure decreases the electrolyzer efficiency.
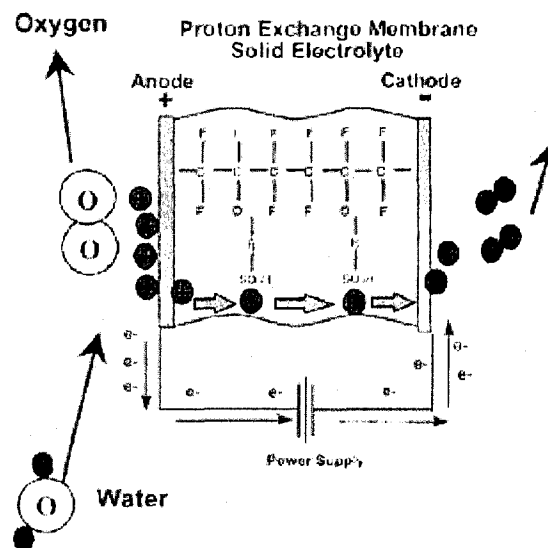
Figure 2. This figure illustrates the process of PEM electrolysis [10].

Among several theoretical studies in the literature regarding solar PV electrolyzer systems, Vanhanen et al. [11] provide a detailed description of a possible stand-alone solar hydrogen energy system. The model included a solar PV array, battery, electrolyzer,

fuel cell, storage tank, and electrical load. The goal of the research was to control each component to optimize the system performance, as well as to show the operational efficiencies of each component of the system. It was found that the overall efficiency of five system configurations was between 3.61% and 3.96%. One of the conclusions of the paper was that matching the voltages and currents in a DC-DC connection is critical to optimizing system performance.

Another theoretical stand-alone system was designed by Lehman and Chamberlin [12], composed of a solar PV array, electrolyzer, hydrogen storage tank, oxygen storage tank, PEM fuel cell, inverter, and compressor. Based on assumptions of solar PV efficiency of 10% and electrolyzer efficiency of 70%, the solar PV array area necessary to provide at least 75% of the power required by a 720 W load was calculated to be at least 60 m^2. Also, the amount of hydrogen storage required to meet at least 80% of the hydrogen demand was calculated using a simulation algorithm that had the system temperature, solar PV current-voltage curves, electrical load, and storage level as inputs. Once again, it was stressed that the current-voltage characteristics of the solar PV array and electrolyzer must be closely matched.

Bilgen [13] showed how a solar PV electrolysis system would be designed and how it would operate in several locations of the United States, and the economical feasibility of such a system. The model created in this work includes a solar PV array and a model of the available solar energy from hourly radiation data, electrolyzer, storage optimizer and solar hydrogen cost. The results of the model show that the overall thermal performance of the system varies from 9.25% to 10.33% for a fixed solar PV array and from 9.85% to

10.85% for a tracking solar PV array. Additionally, the cost of hydrogen production decreases as the available solar radiation increases for a given location.

Mason and Zweibel [14] performed an analysis of the operation of a centralized solar PV electrolysis system to supply one million hydrogen vehicles. This required hydrogen production of 217 million kg of hydrogen, and a solar PV array area of 260 km^2 based on the use of a bi-polar alkaline electrolyzer operating at 67% and a solar PV efficiency of 10%. This paper also showed that the replacement of one million gasoline vehicles with hydrogen resulted in a 90% reduction in CO_2 emissions. Additionally, the authors performed a cost analysis including the cost of each system component, hydrogen pipelines, land, taxes, and the expected operating life of the components to conclude that the levelized cost of hydrogen was $6.48/kg.

In preparation for the HFS described in this thesis, Deshmukh et al. [15] performed a simulation to help design the solar PV array required for the planned electrolyzer and compressor that were to be installed. The solar PV array was assumed to have an efficiency of 12.6%, while the electrolyzer and compressor were expected to use 8.5-9 kW during operation. The array was chosen to provide 14.35 kW, and be grid connected. The array was estimated to be capable of providing enough energy to produce 285 kg of hydrogen. It was found that producing hydrogen during the peak sunshine hours of the day minimized the need for the station to draw power from the electrical grid.

Lehman et al. [16] reported data from an operational solar PV hydrogen system, which was designed to store hydrogen and use a fuel cell in combination with the solar PV energy for an air compressor (load of 660 W). The system operated for over 3900 hours and resulted in an efficiency of 6.2% based on an electrolyzer efficiency of 76.6%

and solar PV efficiency of 8.1%. The type of electrolyzer used was a medium pressure, bipolar, alkaline unit, which was powered with direct DC electricity from the solar PV array.

Another solar PV electrolysis station is described by Vidueira et al. [17]. The station is used to produce hydrogen for two fuel cell buses, and was designed so that the station was energy independent (but still grid connected). The station is controlled such that extra power not used for DC-DC electrolysis is sent to charge batteries used for compression of the hydrogen, and then to the electric grid if the batteries are full. The data used for the design of the station were the average monthly daily irradiance for Madrid, the number of buses, the average traveling distance of the buses (120-130 km/day), the vehicle fuel efficiency (10 km/kg), the electrolyzer output capacity (60 Nm^3/h), and the solar PV array tilt angle (55°). The station was designed to produce the required amount of hydrogen on a day with average daily irradiance based on an entire year. Based on average irradiance conditions over the past 50 years in Madrid, the storage system was sized such that the station has 18 days of autonomy, amounting to 517.5 kg of hydrogen storage (350 bar). The reason was to be 99.5% confident that the station would not have a shortage of hydrogen. Similarly, the battery had to be designed to operate on cloudy days, because it was used to power all equipment except for the electrolyzer. The value obtained for the battery system capacity was 4000 Ah at 380 V. To supply this equipment, based on an expected solar PV efficiency of 13.74%, the array was rated at 528.7 kW, requiring 3110, 170 W solar PV modules.

The results of the research included the amount of energy required per amount of hydrogen produced, the energy consumption of each component in the system, as well as

the output from the solar PV array, and the thermal efficiency of the station. It was found that the station required 73.75 kWh/kg, and an overall thermal efficiency based on the HHV of hydrogen of 9.03%. The authors conclude that the most suitable option for producing hydrogen with no emissions is a grid-connected electrolyzer system.

Chaparro et al. [18] presented a system composed of a solar PV array, batteries, electrolyzer, metal-hydride bed for hydrogen storage, and a fuel cell. The system is designed so that the batteries are charged with the solar PV array and fuel cell, and discharged by the electrolyzer and an application load of 200 W (telecommunication system). The size of the solar PV array was 1.4 kW and the batteries had 20 kWh of storage capacity. A 1 kW PEM electrolyzer was used to produce the hydrogen. In this case the hydrogen is produced at 30 bar and stored in a metal hydride bed, an absorption-desorption type of storage cycle. The system operates such that in the summer months, electricity is supplied to the load by the solar PV array, but in the winter hydrogen is used by the fuel cell to keep electricity going to the load. The operational efficiencies of the solar PV array and electrolyzer were 9.9% and 65% respectively, resulting in overall conversion efficiency between 6-7%. Since this system was a stand-alone system, one significant issue encountered was that when the batteries and hydrogen tanks were full, the energy from the solar PV array was unable to be used. This result indicated that energy management is a critical issue when the efficiency of such a system is evaluated.

Kai et al. [19] have reported on a hydrogen fueling station demonstration project located on Yakushima Island. This station is powered with electricity from hydroelectric dams, and the hydrogen is used for testing fuel cell vehicles on the island. The hydrogen was stored as a compressed gas, with a total storage capacity of 11.25 kg at 351 bar. The

authors monitored the hydrogen storage rate in the system versus the pressure in the

storage tanks, and found that as the pressure increased, the storage rate decreased after

the pressure surpassed 17 bar. This result indicates that more energy is required to store

hydrogen when the storage tanks are at higher pressures. The efficiency of the

electrolyzer during operation was 63%. Since hydroelectricity was used to drive the

hydrogen generation and storage system described by the authors, the overall system

efficiency was higher than those in which PV is the source of electricity. Based on the

HHV of hydrogen, the total energy efficiency of the process was 30%.

Summary of Research Results

Table 1. Summary of Published Results (*Italics* – Assumed Value)

Author	Year	Electrolyzer Power Production Requirement (kWh/kg)	Electrolyzer Efficiency (%)	Power Source	Solar Array Efficiency (%)	Overall Efficiency (%)
Lehman	1991	*56.3*	*70.0*	*PV*	*10.0*	*7.0*
Vanhanen	1994			PV		3.61-3.96
Lehman	1997	51.4	76.6	PV	8.1	6.2
Bilgen	2000			*PV*		*9.85-10.85*
Viduera	2003	*73.8*	*53.4*	*PV*	*13.7*	*9.03*
Chaparro	2005	60.6	65.0	PV	9.9	6.0-7.0
Conibeer	2006	*60.6*	*65.0*	*PV*	*13.5*	*8.8*
Ivy	2006	*53.0*	*74.0*	*PV*	*10.0*	*7.4*
Kai	2007	62.5	63.0	Hydro	N/A	30.0
Mason	2007	*58.8*	*67.0*	*PV*	*10.0*	*6.7*

CHAPTER 2

HYDROGEN FILLING STATION DESCRIPTION

Phase II Station Configuration

The original HFS installation constituted Phase II of the project, and was installed in

Las Vegas in January 2007. Figure 3 is a picture of the station taken shortly after its

construction, with the equipment labeled. This station configuration was designed to

support two small utility vehicles that were converted to run on hydrogen [20]. The

station is composed of a low pressure and high pressure electrolyzer, an intermediate

buffer tank, a compressor for each electrolyzer, and a dispensing unit for storing and

dispensing the hydrogen to vehicles.
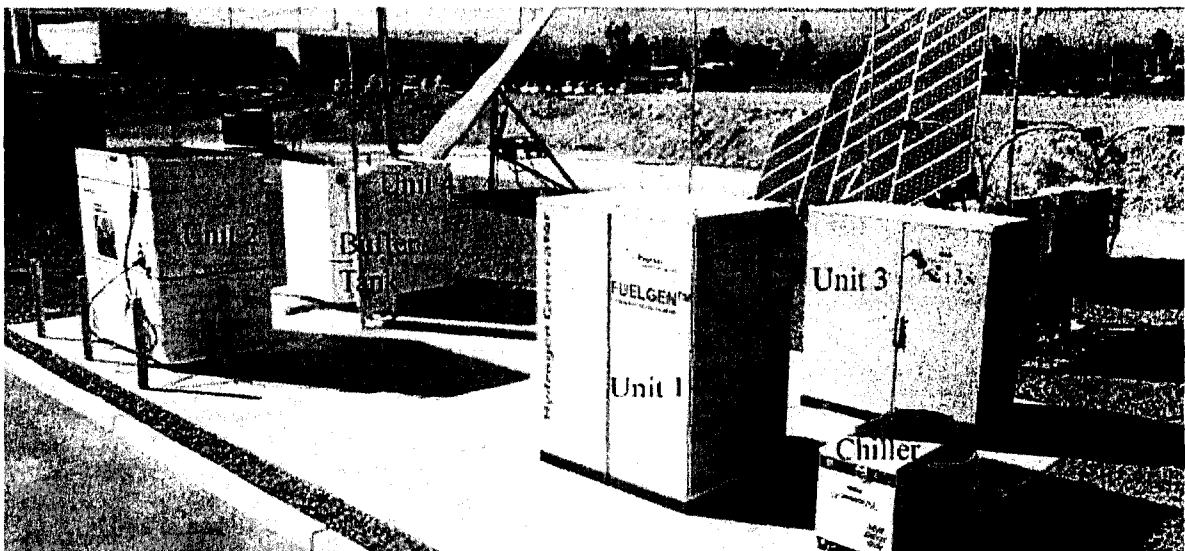
Figure 3. Phase II of the HFS project with equipment labeled.

Unit 1 is a Proton Energy Systems FUELGEN HG-1® renewable PEM electrolyzer, which is capable of producing 2.0 kg of hydrogen per day (0.083 kg/h). The hydrogen is produced at 14 bar (~200 psi), and during operation it uses approximately 7.5 kW. Unit 3 is an experimental Proton Energy Systems FUELGEN HG-2® PEM Electrolyzer which is capable of producing 0.25 kg of hydrogen per day (0.0104 kg/h) at a pressure of 70 bar (1015 psi). Since this unit generates hydrogen at a higher pressure, it reduces the energy required to further compress the hydrogen to the storage pressure required for filling the vehicles. Unit 4 is an Air Products Hydro-Pac Compressor, which was used to compress and store the hydrogen from the experimental Unit 3 electrolyzer. The chiller at this station was required by the high pressure cycle to cool the compressor during operation. It has 2 kg of hydrogen storage capacity at 430.9 bar (~6250 psi). Unit 2 is an Air Products Series 100E compression, storage, and dispensing module, with 6.5 kg hydrogen storage capacity. This unit compresses the hydrogen to 430.9 bar (~6250 psi) with a single stage Pressure Dynamic Consultants (PDC) diaphragm compressor, and stores it in six storage tanks, each of which has a volume of 0.042 m^3 (1.47 ft^3). The tanks are emptied into a vehicle with a "cascade" system using automatic hydrogen-operated valves, so that three banks of two tubes are emptied sequentially to fill the vehicle, to maximize the utility of the stored hydrogen. The buffer tank serves as an intermediate low pressure storage location between Unit 1 (generation) and Unit 2 (compression/dispensing). This decouples the electrolyzer from the compressing unit, so that each unit can operate independently. Water and hydrogen flows for the Phase II station are shown in Figure 4. Assuming the station is full of hydrogen, after hydrogen is dispensed into a vehicle, the compressor begins to compress hydrogen from the buffer

tank into its storage tanks at its nominal flow rate of 0.101 kg/h. When the level of the

buffer tank drops below the set point pressure of 13 bar (188.5 psi), the electrolyzer

begins to input water and electricity and output hydrogen, to refill the buffer tank.
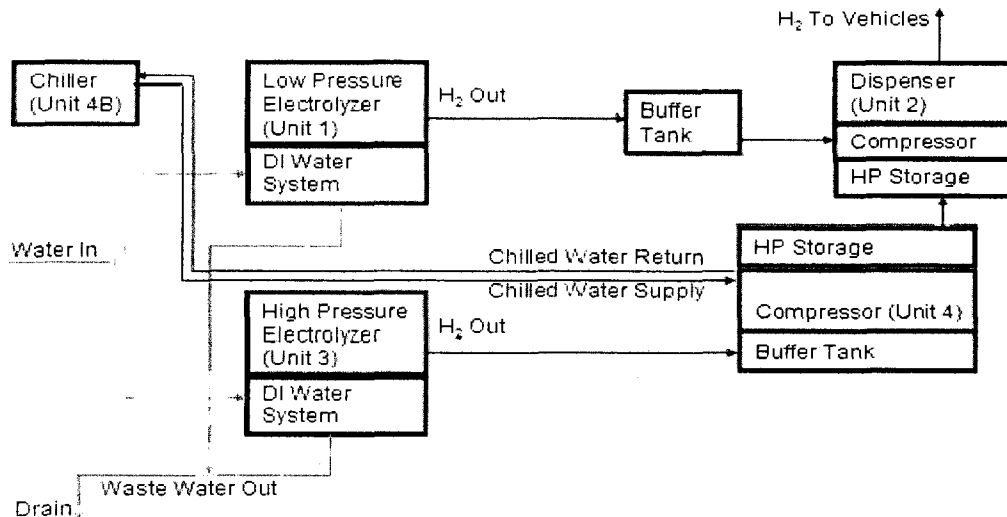
Figure 4. Water and Hydrogen Flow at the HFS.

The system is powered by a grid connected photovoltaic system, which is made up of

four single-axis tracking units shown in Figure 5. Each tracker is tilted at 30 degrees, and

consists of 24 Sharp 175 Watt monocrystalline panels (Model NT-175U1). The total

system output is 16.8 kilowatt electric (kWe) DC or 14 kWe Alternating Current (AC).

The estimated annual energy generation is 37,000 kilowatt hours (kWh), and the

estimated efficiency is 12.6%. A Xantrex Model PV-15208 inverter was installed to

convert the DC power to AC, to allow grid connection of the system.
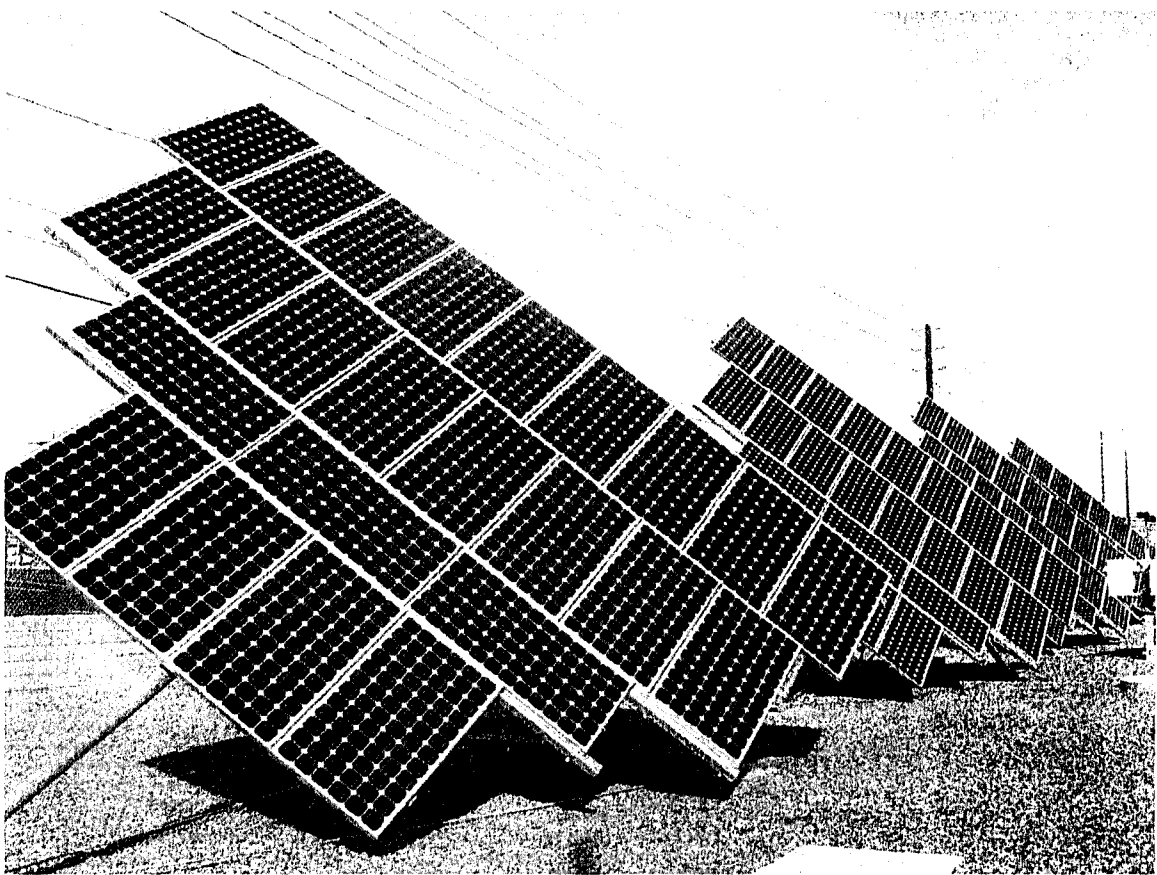
Figure 5. Solar PV system installed to provide power for the HFS.

The system is connected to the grid, and a net metering agreement with Nevada

Power Company (NPC) allows excess power generated by the solar PV array to go to the

grid when the system is not generating hydrogen. Also, the hydrogen generation and

compression equipment can draw power from the grid when the system is generating

hydrogen on cloudy days or at night. The meter is capable of monitoring power flow in

both directions, and a renewable energy meter installed at the station allows for on-site

monitoring of the solar PV array production. A diagram describing how electricity flows

through the system is shown in Figure 6.
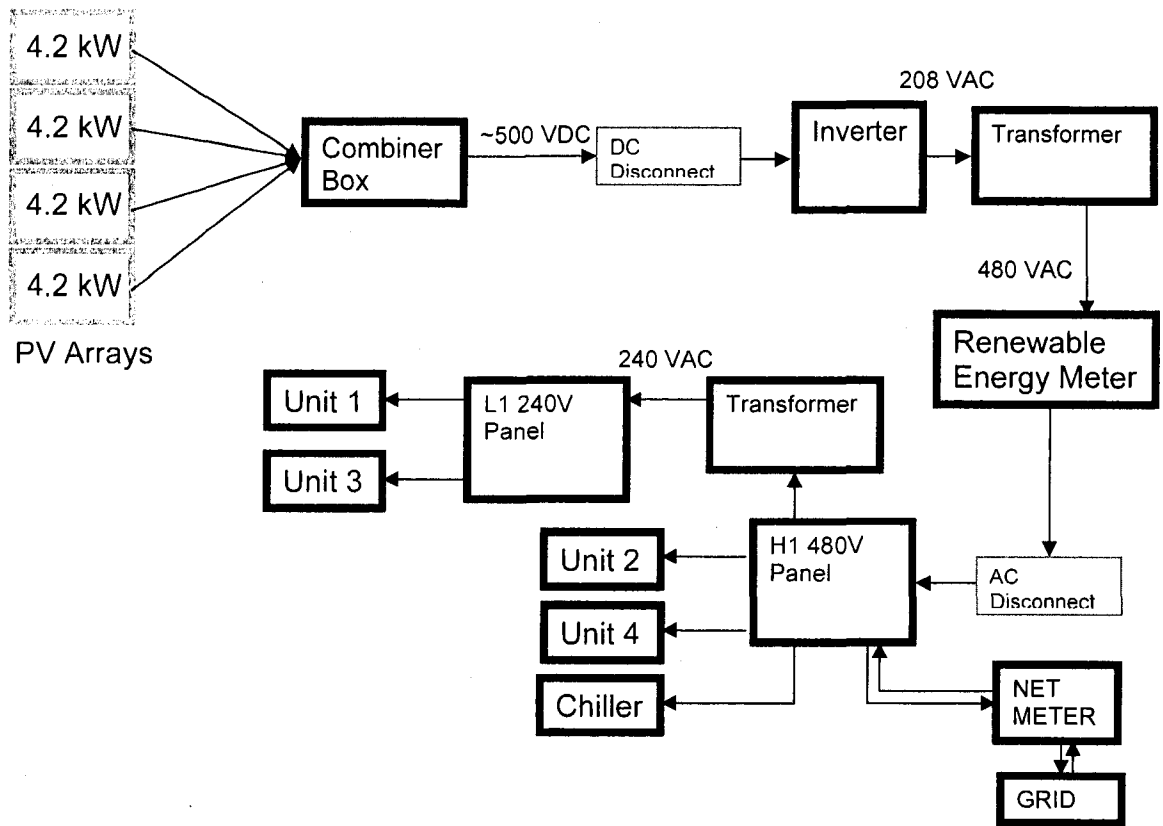
Figure 6. Electricity diagram of the Phase II HFS, note the Net Meter.

Phase III Station Configuration

In January 2008, the HFS was upgraded in order to increase its hydrogen production

capability. The additional hydrogen will be used by a newly converted Ford F-150 pickup

truck [21], which will be used as a meter-reading vehicle at the LVWWD. As shown in

Figure 7, all of the original units and tanks were removed, and the upgraded station is

composed of a new electrolyzer, chiller, buffer tank, and compressor/dispenser unit.
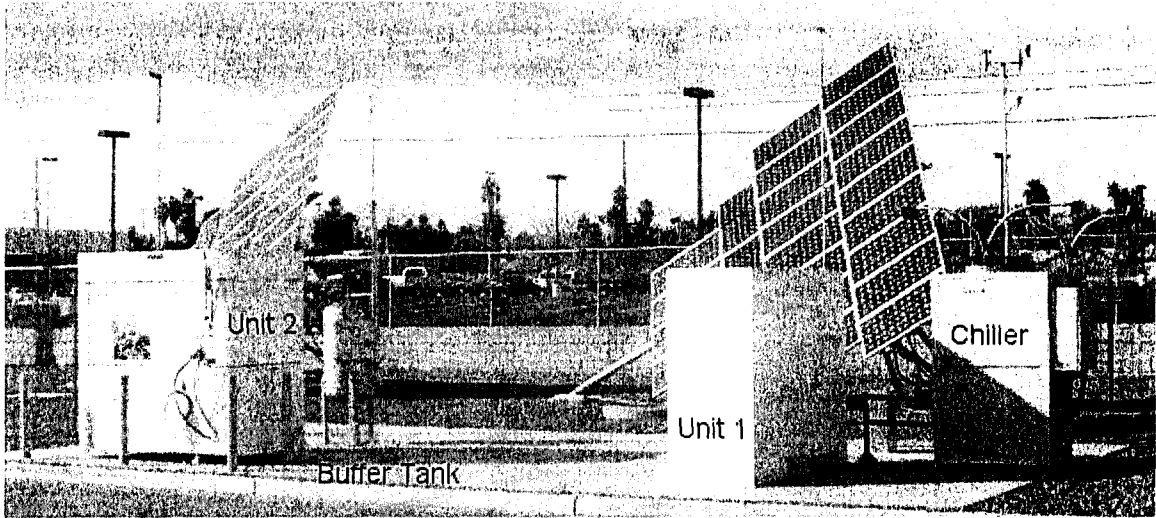
Figure 7. Picture of Phase III of the HFS project with equipment labeled.

To increase the amount of hydrogen produced at the station, Unit 1, a Proton Energy Systems FUELGEN 12 ® PEM Electrolyzer, was installed. The electrolyzer has a 12.94 kg per day (6 Nm³/hr) production capacity, and an output pressure of 30 bar (435 psi). A chiller (Unit 1a) is used to maintain the operating temperature of the PEM electrolyzer stack during hydrogen production. The capacity of the chiller is 10 tons, and R-134a is used as its refrigerant. Unit 2 is a new Air Products Series 100E dispenser that includes a compressor and storage tanks. The capacity of storage tanks is 6.5 kg of hydrogen at 430.9 bar (6250 bar). The Phase III station uses the buffer tank as the intermediate hydrogen storage area in the same way that the Phase III station operated. Figure 8 shows the updated water and hydrogen flow diagram for the Phase III station.

18
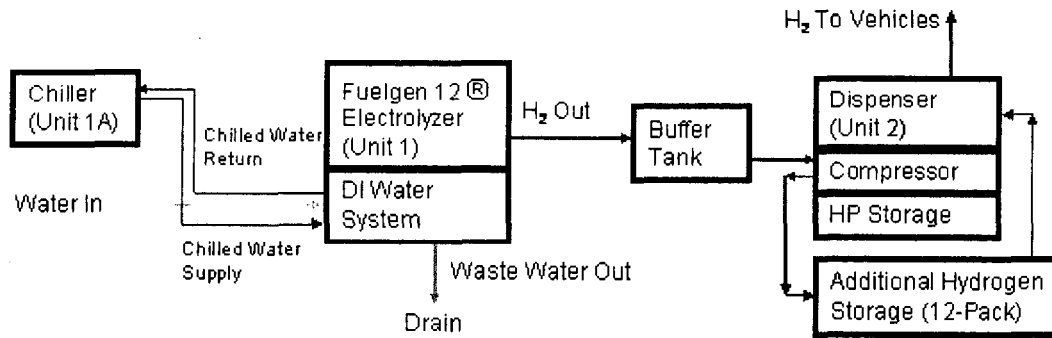
Figure 8.   Water and hydrogen flow at the Phase III HFS.

The Phase III station electrical diagram is different as well. The electrolyzer requires 480 VAC input, instead of the 240 VAC required by the Phase II electrolyzers. Additionally, an auxiliary heater inside the new electrolyzer requires 240 VAC. The station remains grid connected, and the updated electrical diagram is shown in Figure 9.
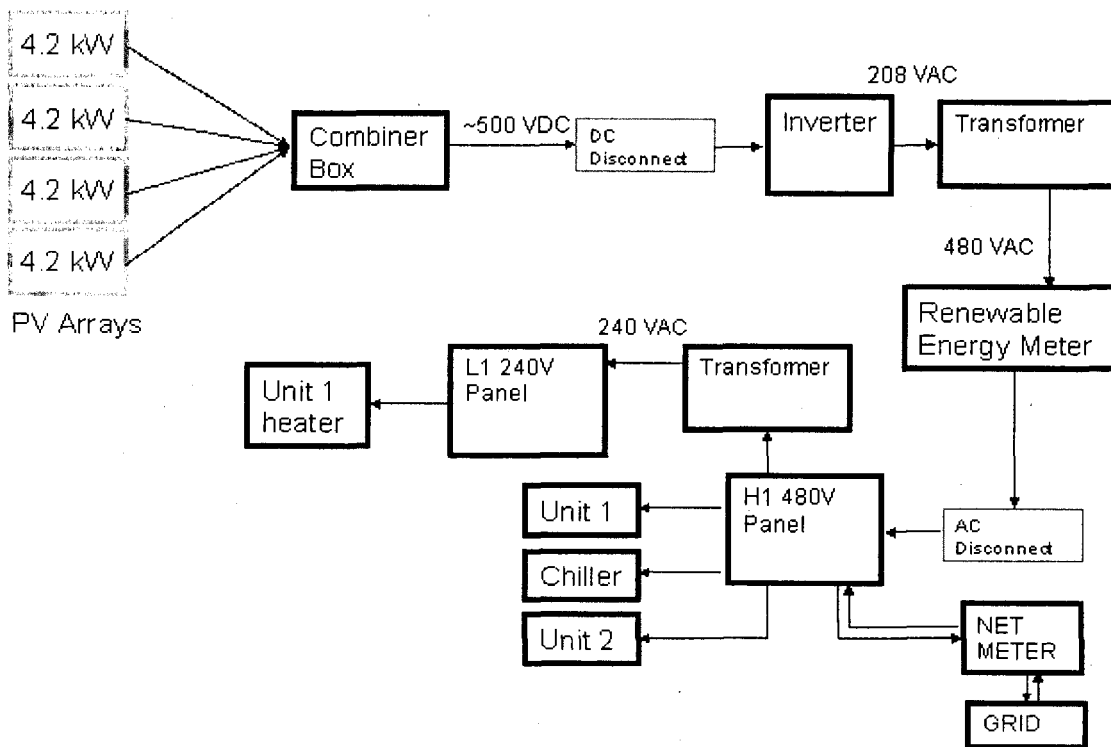
Figure 9.   Electrical diagram of the Phase III HFS.

19

CHAPTER 3

DATA ACQUISITION SYSTEM

To monitor the performance of the equipment at the HFS, a data acquisition system

(DAS) was installed. Sensors were placed at the station to monitor weather conditions,

energy use by the HFS equipment, energy generated by the solar PV array, and the

amount of hydrogen produced at the station. For data collection, a Campbell Scientific

Incorporated (CSI) Model CR10X programmable data logger was installed, shown in

Figure 10. This data logger has twelve single ended channels, two pulse counters, three

excitation channels, eight control ports, and a 2MB extended memory. The data logger

requires 12 V DC and a phone line for communications.
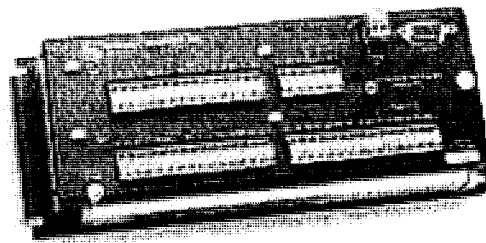
Figure 10. CSI Model CR10X data logger.

The data logger is powered by a CSI Model PS100 12 V power supply, with charging

regulator and a 7 Ah backup battery connected to a CSI Model 9591 110 V AC to 18 V

DC power supply, shown in Figure 11.

Figure 11. PS100 12 VDC power supply with charging regulator and battery.

For communications the data logger is connected to a CSI Model COM 210 9600 bits per second telephone modem (Figure 12) which is connected to a telephone line. This allows the data to be downloaded and monitored remotely from a computer with CSI Loggernet software.
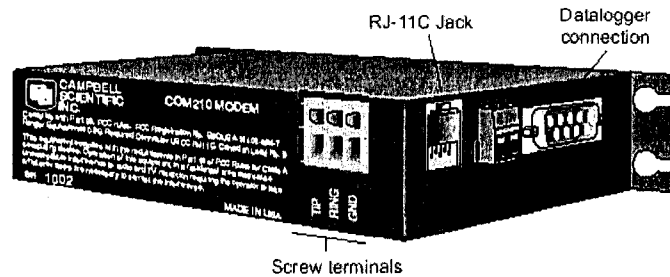
Figure 12. CSI Model COM210 telephone modem.

To add monitoring channels to the data logger, the CSI Model AM16/32 relay multiplexer shown in Figure 13 was added to the data logger for an additional 32 analog sensor inputs. Additionally, the CSI Model SDM-SW8A 8 channel switch closure input module shown in Figure 14 was installed to add 8 channels of switch closure or voltage pulse inputs.
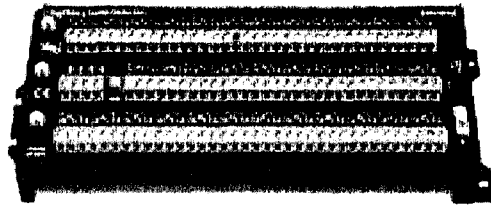
Figure 13. CSI Model AM16/32 16-channel or 32-channel relay multiplexer.
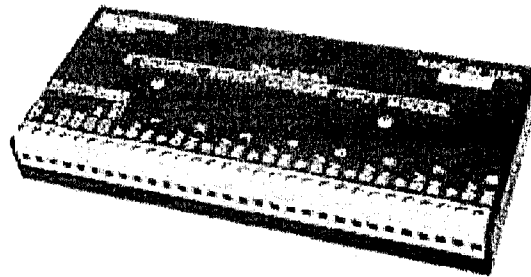
Figure 14. CSI Model SDM-SW8A 8-Channel switch closure input module.

Electrical power is measured using Continental Control Systems (CCS) WattNodes (model numbers are determined by voltages and phases), which are Watt/Watt hour transducers. These are connected to split core current transformers, which are installed around the wires located in the electrical panels. The pulse outputs from the WattNodes are measured in the switch closure input module. The WattNodes require connections into the phases that are being measured as shown in Figure 15. Electrical power to be measured will include power generated by the photovoltaic systems, power used by the electrolyzers and chiller, power used by the compressors and power from the grid. Since WattNodes can only measure power in one direction a second WattNode with current transformers is required on the mains to measure both directions of power flow during periods when the photovoltaic system is supplying power to the grid.

Three Phase, Four Wire
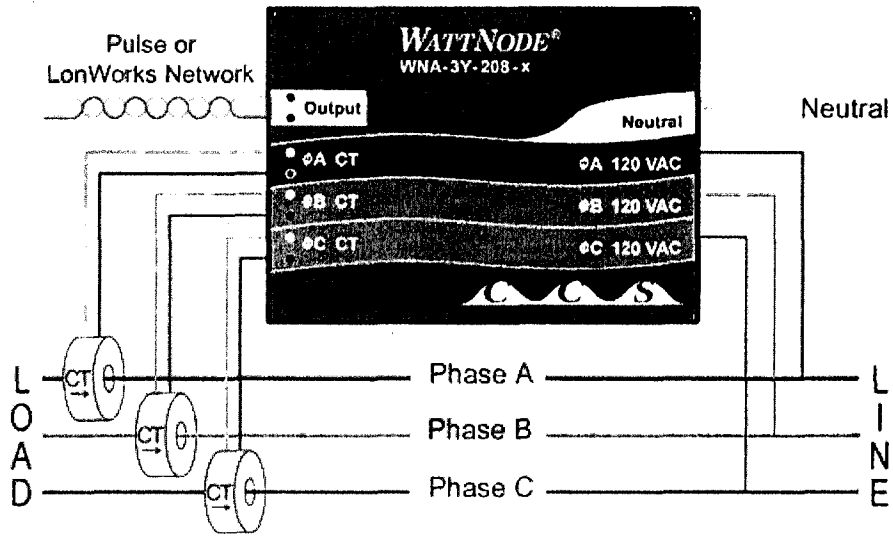
Figure 15. Typical CCS WattNode three phase-four wire wiring diagram
(http://www.ccontrolsys.com/downloads/WattNodePlusDataSheet.pdf).

Based on the current rating of each piece of equipment, the appropriate current

transformer that delivers the signal to each WattNode was mounted on each phase of the

voltage lines as shown in Figure 16.
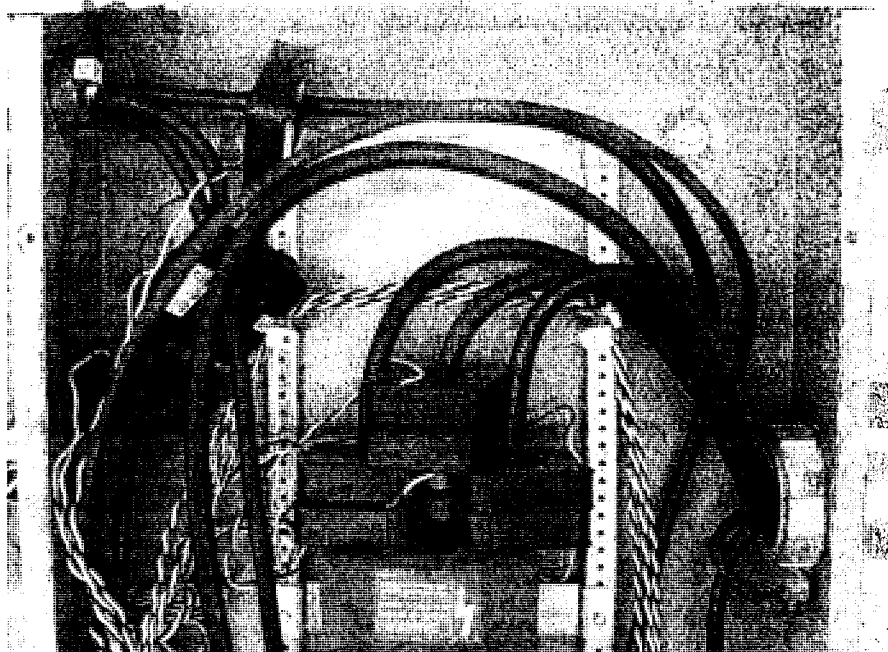
Figure 16. Current transformers installed on voltage lines.

The data logging equipment is installed on the electrical power rack adjacent to the

two voltage panels, as shown in Figure 17. A CSI Model ENC 16/18-10628 weather

resistant enclosure houses the data logger, power supplies, modem, multiplexer, switch

closure module, and WattNodes. This enclosure is rated at NEMA 4X modified for cable

entry.
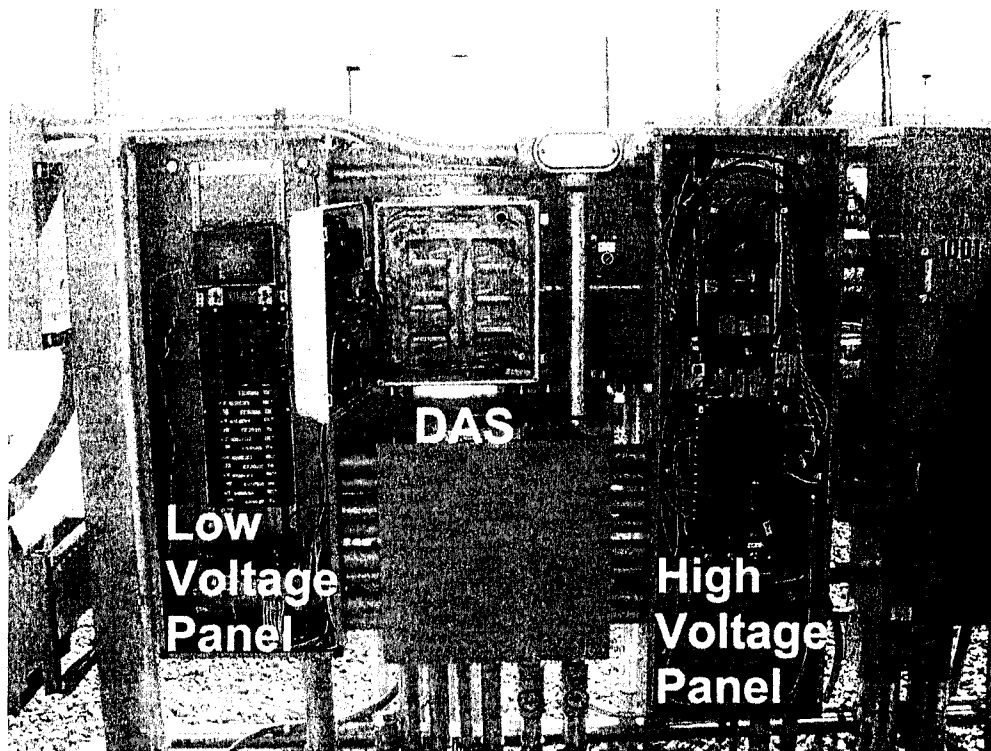
Figure 17. Electrical rack at the HFS, with DAS in the center.

Figure 18 shows how the data logging equipment is installed in the enclosure. The

required signal wires from the high voltage and low voltages are brought into the box for

the WattNodes, which are mounted on the back wall of the box and covered with a PVC

shield to protect users from the high voltages in the enclosure. A steel sheet was mounted

inside the door, to provide a platform for the CSI data logging equipment. The wiring

diagram for this DAS can be found in the appendix.
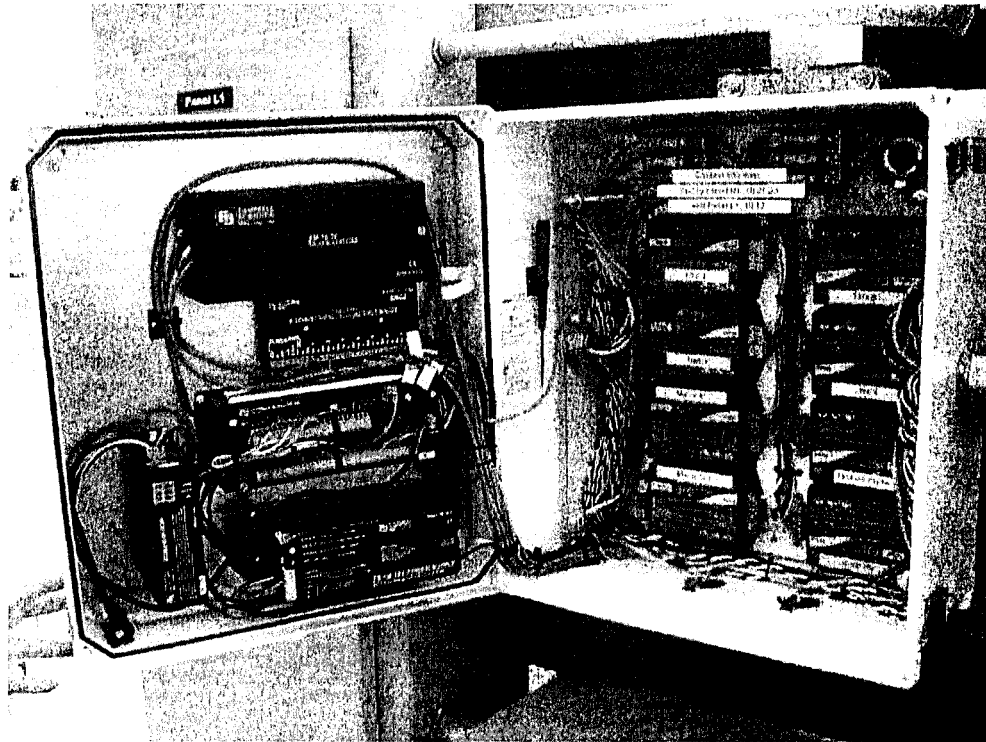
Figure 18. CSI Enclosure with data logging equipment.

To monitor the wind speed and direction, a R.M. Young model 03001 Wind Sentry Set was installed. This unit has an uncertainty of ±0.5 m/s. Ambient temperature and relative humidity are measured using a Vaisala Model CS500-L40 temperature and relative humidity probe with radiation shield. It is capable of accuracies of ±0.2-0.8 °C for temperatures of 0-60 °C, and ±3% for relative humidity. The wind and temperature sensors were installed on a rigid pole at a height of 4.5 m, and mounted to the electrical rack next to the low voltage panel (Figure 19).
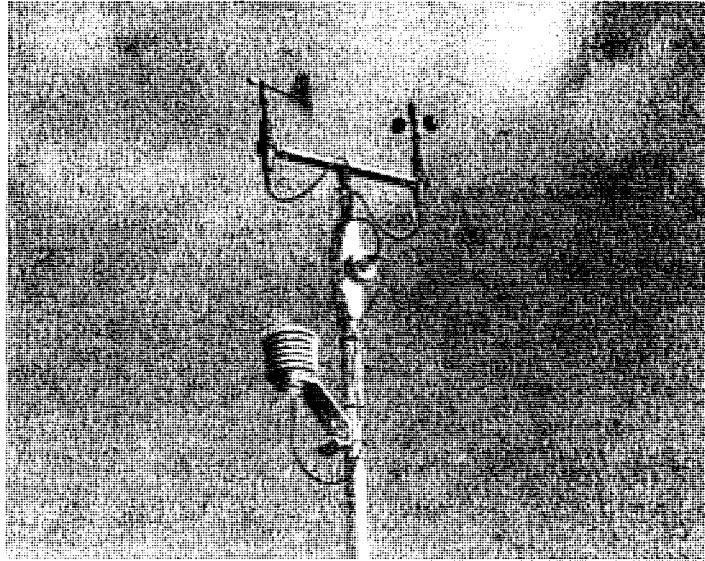
Figure 19. Wind and Temperature Sensors Installed at the HFS.

Solar flux is measured using a LI-COR Model LI200X silicon pyranometer which measures wavelengths of radiation between 400 and 1000 nm, and has an absolute error of ±3% of its reading. It is mounted on and oriented in the same·plane as the tracking photovoltaic panels, as shown in Figure 20.
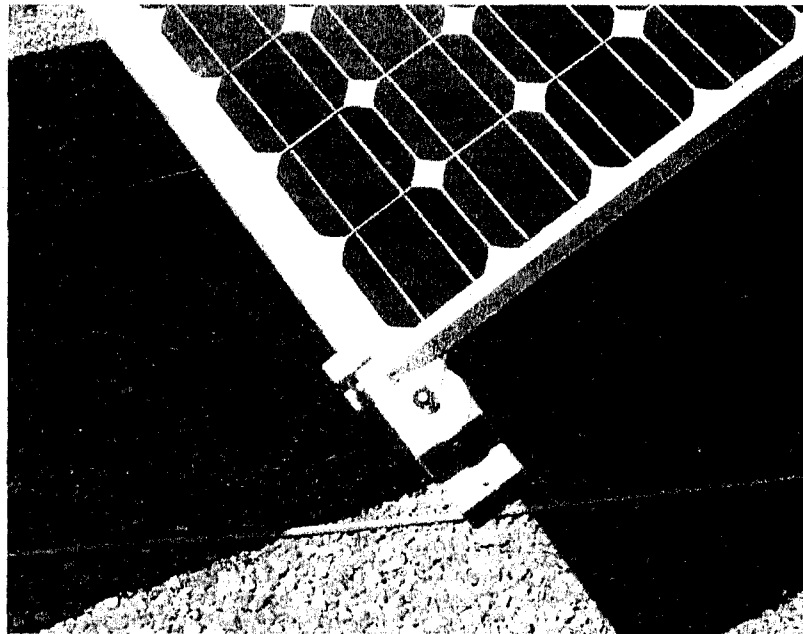
Figure 20. Pyranometer installed on tracking unit.

For the Phase III HFS, a hydrogen mass flow meter was installed in order to measure the mass flow rate of hydrogen generated at the station. A MicroMotion Model CMF010M, Coriolis ELITE sensor was installed directly in the product line of the electrolyzer, next to the blower as shown in Figure 21. The output signal from the flow meter is a RS-485, four-wire signal, which runs underground and connects to a transmitter located on the electrical rack. The sensor is capable of measuring the hydrogen mass flow rate with an uncertainty of ±0.03%.
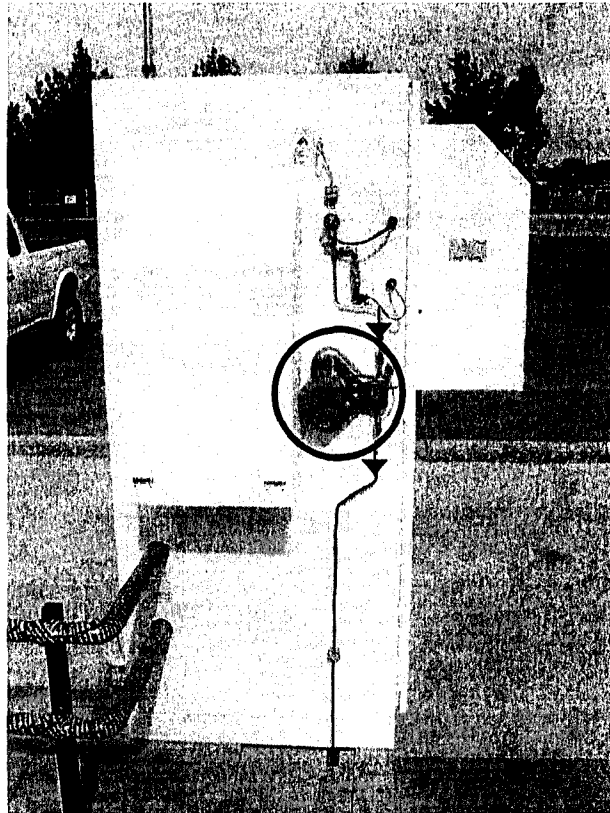
Figure 21. Hydrogen mass flow meter installed on Unit 1.

The transmitter shown in Figure 22 is a Micro Motion Coriolis MVD multivariable flow and density transmitter, Model 2700. It receives the data signal from the flow meter, and outputs a 4-20 mA signal as well as pulse output for data collection. Additionally, the

transmitter has a digital display that reports the mass flow rate in kilograms per minute in real time. The pulse output from the transmitter is connected to the CR10X data logger as shown in the appendix. The transmitter is configured so that each pulse represents 0.0167 kg of hydrogen generated.
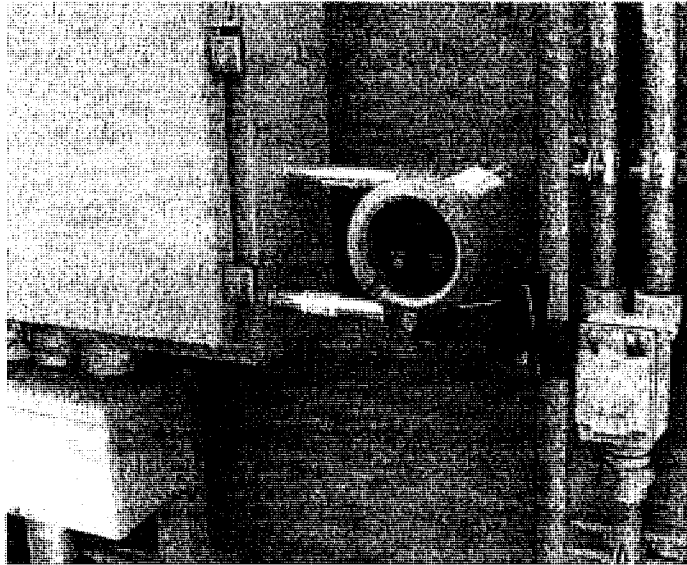
Figure 22. Hydrogen mass flow transmitter mounted on electrical rack.

The data from each sensor installed at the HFS is collected and stored by the data logger every minute. The data logger is programmed to store each piece of data such that the value is appropriate for the signal. For example, the temperature reported for each minute is an average reading over that minute, while the amount of energy produced by the solar PV array is a total amount of energy produced during that minute. A program was written to perform these operations with the CR10X data logger, and the program code is available in the appendix.

The CSI Loggernet software is then used to contact the data logger via the CSI modem, and download the data for archiving and analysis. To provide real-time

28

monitoring of the HFS, CSI Real-Time Data Monitoring Software (RTDM) was used.

This software allows the user to create several different types of plots, based on the data

collected by Loggernet from the CR10X data logger. Each three hours, a computer with

the Loggernet software makes a connection to the CR10X at the HFS, downloads the last

three hours of data, and the RTDM software then updates the user-created plots. An

example of a plot generated by RTDM is shown in Figure 23.
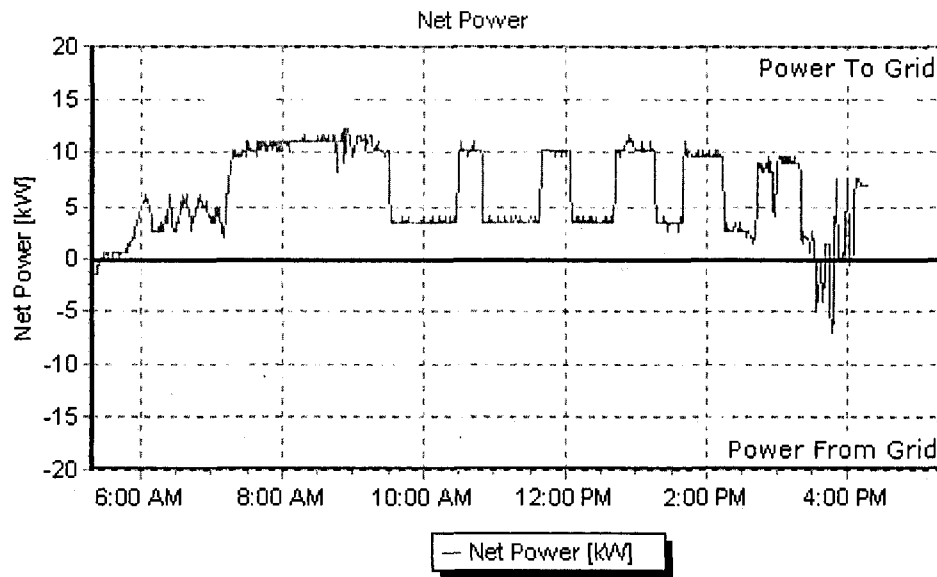
Figure 23. Sample plot generated by RTDM software.

In addition to providing real-time data to UNLV for performance monitoring, the

RTDM software is able to generate plots like the one shown in Figure 23 for display on

the internet. This allows the public to view the conditions and performance of the station

by logging on to www.hydrogen.unlv.edu/HFS.html. A screenshot of this website can be

seen in Figure 24.
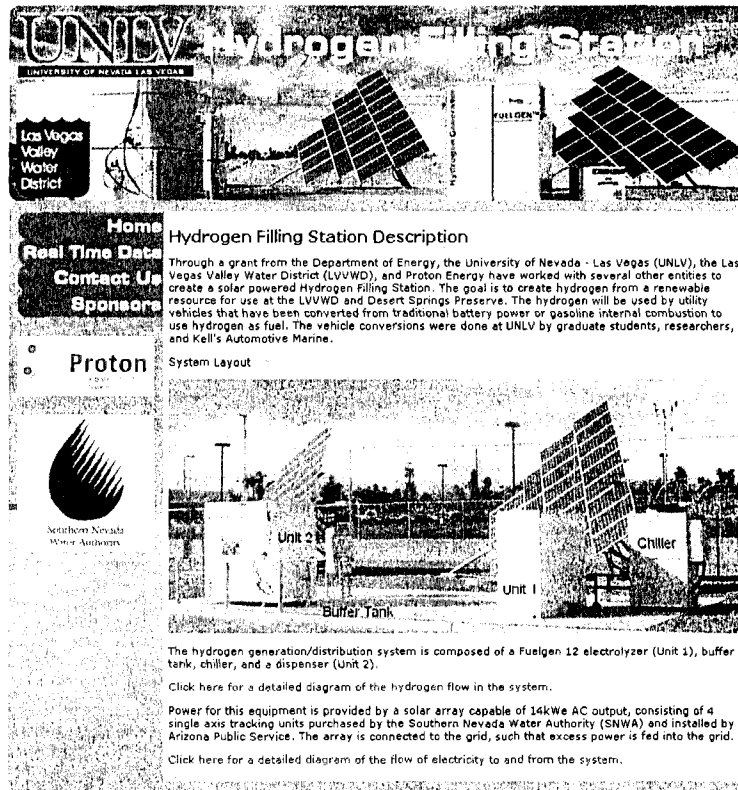
Figure 24. HFS website screenshot.

To provide a daily summary of the station's performance to UNLV and the LVVWD,

as well as Proton Energy Systems and Air Products, Inc., a computer program was

written using MATLAB. The summary program uses Windows Task Scheduler to run

each morning, in order to analyze the previous day's data to provide a text file of the

daily performance of the HFS. Data included in the output file includes the energy use of

each piece of equipment, average and maximum wind speeds and temperatures,

maximum and total solar PV array power and energy outputs, and the total amount of

hydrogen produced. The data is available as a comma delimited data file, and the

program also organizes the total energy use at the HFS into a bar chart describing the net

energy produced or used during the day. A sample month of the daily data bar chart is

shown in Figure 25.
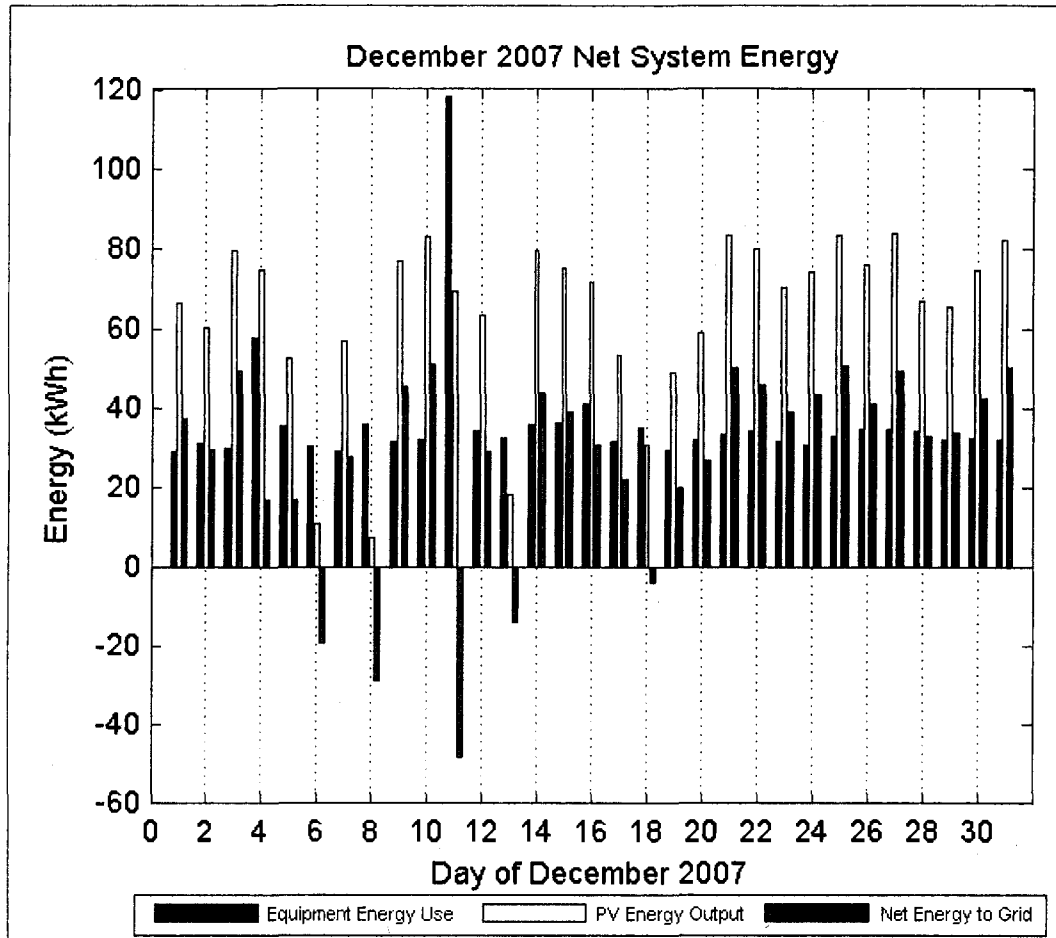
Figure 25. Sample monthly plot of net system energy.

To verify that the data collected at the HFS was accurate, each sensor was monitored

and compared with a similar, previously verified sensor. Weather data such as ambient

temperature, humidity, wind speed, and available solar radiation were compared to data

from other weather stations in the Las Vegas area, and found to be in agreement. Output

from the WattNodes was verified by monitoring each piece of equipment as it operated

with an Amprobe Model DM-II PRO data logger/recorder, which provided real-time

information power use of the equipment. This data was compared to the corresponding

WattNode output, and it was found that the WattNodes provided the true energy use of

the HFS equipment.

CHAPTER 4

EXPERIMENTAL RESULTS

Phase II Hydrogen Filling Station Operation

The Phase II HFS was in operation for almost one year, of which there were 5 months of error-free continuous operation that provided valuable data regarding the performance of the station. Among the important data collected were the energy output from the solar PV array, its efficiency, the energy used by the electrolyzer and dispensing unit during production and compression of hydrogen, and net energy production at the station. Table 2 provides a summary of the solar PV performance over the five month period from May to September 2007, as well as the total amount of energy that was exported to the grid.

Table 2.	Phase II Five Month Station Performance
PV System Efficiency (After Inverter)	9.85%
Total PV Energy	18.64 MWh
Total Energy to Grid	11.13 MWh
Number of Days Generating Hydrogen	~15

As shown in Table 2, there were only about 15 days when hydrogen was generated at the station, due to the fact that the vehicles were still in their conversion and testing phase. The solar PV array produced a total of 18.64 MWh during the five months, of which 11.13 MWh went to the grid as excess energy. The solar PV array performed at an

average efficiency of 9.85% over the five month period, which is the based on the energy

output from the panels divided by the total available energy incident on the panels'

surface, as shown the following equation:

$$\eta_{c,PV} = \frac{E_{PV}}{I_T A_{PV}}$$ (1)

where A_{PV} is the area of one panel and I_T is the incident radiation in W/m^2, which is

measured by the silicon pyranometer mounted on the tracking unit, as shown in Figure

20. Based on the measurements of incident radiation from the silicon pyranometer and

power output from the solar PV array, a plot similar to the one shown in Figure 26 was

generated in real time. By allowing the scales of PV output and incident radiation to

automatically adjust on the same plot, the performance of the array can be examined in

detail. For example, as shading causes the reading from the pyranometer to drop, the

power output from the solar PV array should drop in the same proportion. Figure 26

shows that at 3 p.m. it appears some of the solar PV array is being shaded, as shown by

the pyranometer reading's divergence from the solar PV array power output.
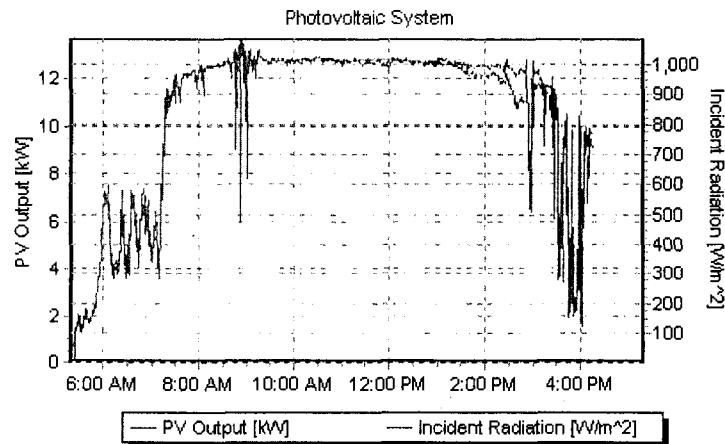
Figure 26. PV output and incident radiation with sliding scales.

The solar PV efficiency was affected by the ambient temperature at the HFS. Figure

27 shows how the average monthly ambient temperature adversely affected the

performance of the solar PV array. It is shown that an average monthly temperature

increase of 8.1° C from May to July decreased the solar PV efficiency by 0.365%. The

result is a drop of 0.045%/°C, which agrees with values obtained from literature for

monocrystalline solar panels [22].
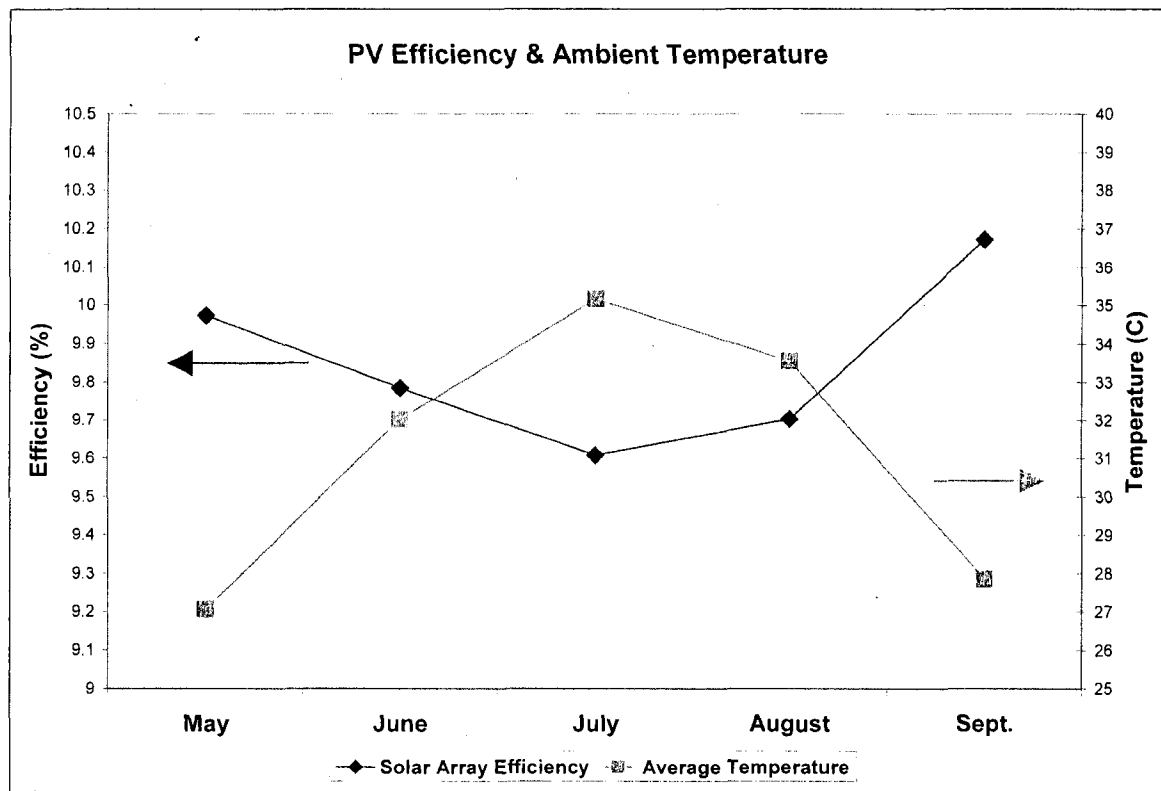
Figure 27. Solar PV Efficiency and Ambient Temperature for May –Sept. 2007.

Since one of the goals of this research was to measure the amount of energy required

to produce hydrogen, testing was performed at the Phase II HFS to determine this

parameter. A converted hydrogen vehicle was filled and driven several times, and the

total amount of hydrogen generated was calculated by measuring the temperature and

pressure of the vehicle's hydrogen tank, as well as the temperatures and pressures of the tanks in Unit 2 (compressor/dispenser). Testing took place from July 27 – July 29, 2007, and was performed at the LVVWD. During the vehicle testing, a total of 3.104 kg of hydrogen was dispensed into the vehicle, and the energy use of the electrolyzer and compressor/dispenser was measured. As shown in Figure 28, the electrolyzer and compressor/dispenser operated for three days in order to refill the storage tanks. During operation, the electrolyzer used between 7 and 8 kW, and the compressor/dispenser used around 1 kW of power. The solar PV power produced during the three day testing period is shown in Figure 29.
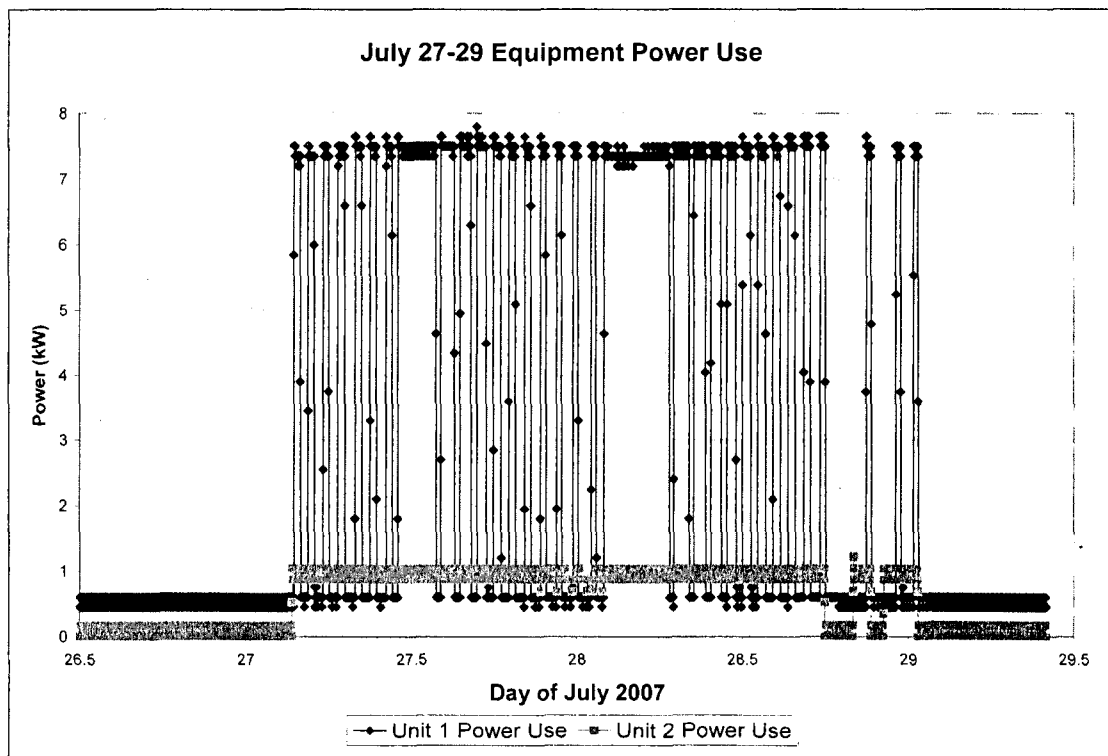
Figure 28. HFS equipment power usage on July 27-29.

35
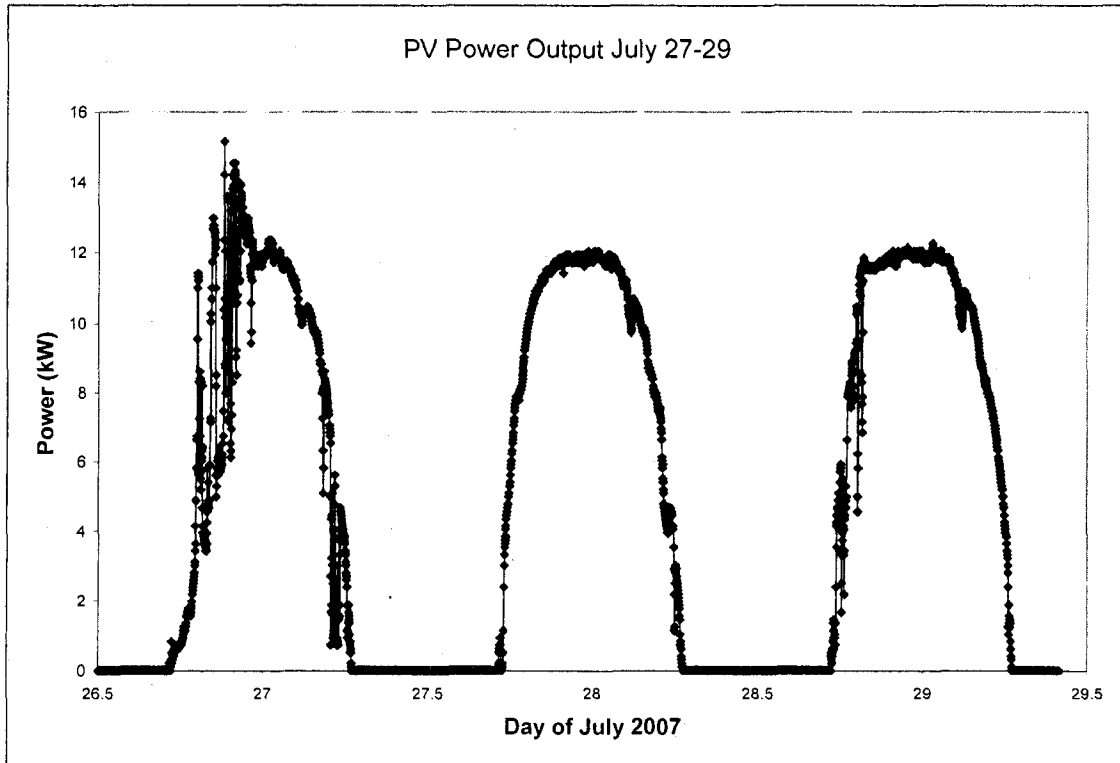
Figure 29. PV array output for 3-day test.

When the power plots shown in Figures 28 and 29 are combined, the net system power output or input can be observed. Figure 30 shows that when the HFS was generating hydrogen during the same hours that the solar PV array was producing power, there was a surplus of power produced at the station. This extra power went to the grid, while power used by the HFS from late afternoon through the night and to the early morning of each day was from the grid.
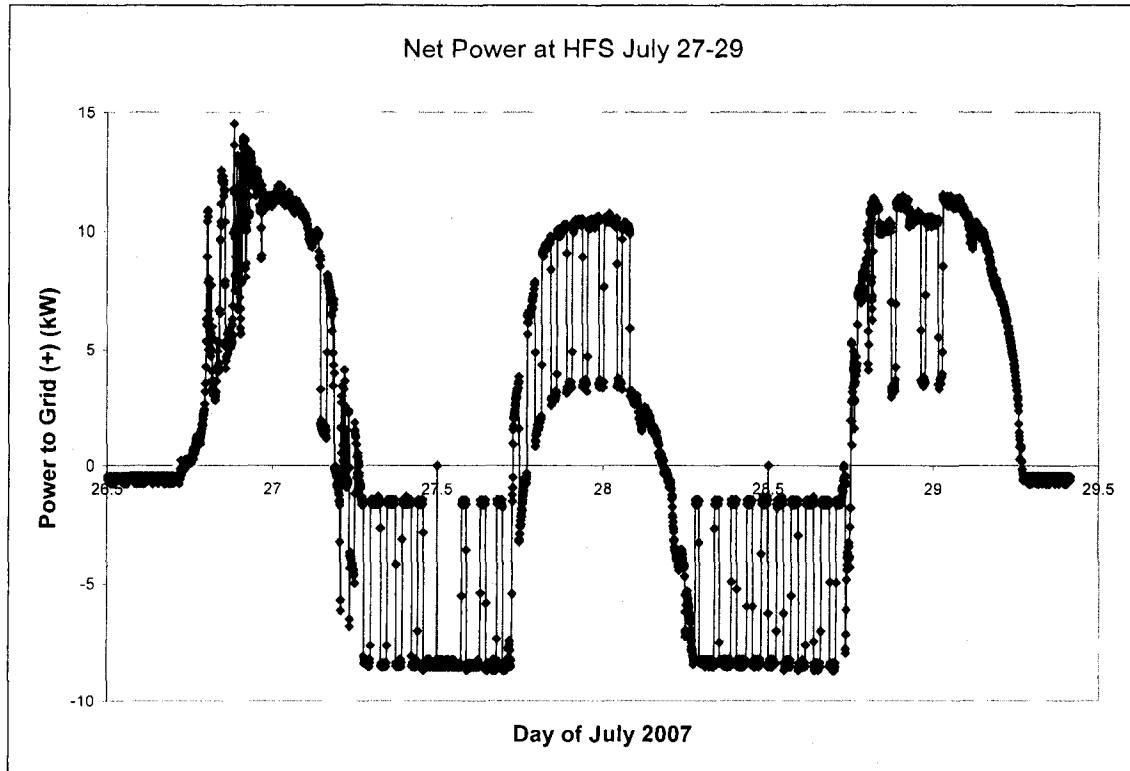
Figure 30. Net power to/from grid during 3-Day Test.

Table 3 provides a summary of the amount of power consumed by the HFS

equipment while producing the hydrogen over the three day test period.

Table 3.	Phase II Three Day Test Results
Mass Generated by HFS	3.104 kg
Energy Consumed	226.85 kWh
PV Energy Produced	357.53 kWh
Production Power Requirement	73.08 kWh/kg
HFS Hydrogen Production Efficiency	53.9 %

The vehicle's tank was filled 9 times, for a total of 3.104 kg of hydrogen, and an

average tank fill of 0.388 kg of hydrogen. The solar PV array's energy output was 357.53

kWh, which resulted in a net energy output of 130.68 kWh at the HFS during the three

day test period. From this data, it is possible to calculate the efficiency and the energy

requirements of the HFS. To calculate the efficiency of the HFS, the amount of hydrogen

37

produced is multiplied by its HHV and divided by the amount of energy consumed during production. The HHV of hydrogen is 39.38 kWh/kg, so the total amount of energy contained in the hydrogen that was produced by the station was 122.24 kWh. Therefore, the efficiency of the HFS hydrogen production was found to be 53.9%. When combined with the calculated value of solar PV efficiency for July, this results in an overall solar energy conversion of 5.17%, which compares well with the values summarized in Table 1 of the literature review.

By dividing the amount of energy required to produce the hydrogen by the amount of hydrogen produced, a value of 73.08 kWh/kg hydrogen was obtained from the three day test. Based on this value, and the amount of energy that was produced by the solar PV array over the five months of operation described above (18.64 MWh), a total of 255 kg of hydrogen could have been produced by solar power alone during those five months. If the tank requires 0.388 kg of hydrogen per fill, this is enough hydrogen to fill the vehicle's tank over 657 times.

While only a small amount of performance data from Unit 3 was collected, it was valuable to the manufacturer. Several design issues were recognized, including a problem with cooler ambient temperatures causing freezing and the production of "wet hydrogen", hydrogen with an unacceptably high water content, due to the orientation of the hydrogen/water separation tank. Due to these issues, this thesis will not present performance data from Unit 3 and the Unit 4 compressor.

Phase III Hydrogen Filling Station Operation

The Phase III HFS has provided over five months of continuous data as of the writing of this thesis. The performance of the upgraded Phase III equipment from the months of

January to May 2008 is summarized in Table 4. Solar PV array efficiency was higher during this five month period, compared to the months of May to September 2007 during Phase II operation, although total array output was lower. Due to the fact that the converted hydrogen vehicles were still being completed, hydrogen was only used five times during this five month period.

Table 4.	Phase III Five Month Station Performance
PV System Efficiency (After Inverter)	10.32%
Total PV Energy	16.75 MWh
Total Energy Sold to Grid	9.72 MWh
Number of Days Generating Hydrogen	~5

The solar PV efficiency was again affected by the ambient temperature during the five months of operation considered. Figure 31 shows how the average monthly ambient temperature adversely affected the performance of the solar PV array. In this case, an average monthly temperature increase of 16° C from January to May decreased the solar PV efficiency by 0.283%. The result is a drop of 0.018%/°C, which compared to the drop of 0.045%/°C shows that the change in temperature from January to May 2008 had less of an impact on PV performance than the change in temperature from May to July 2007.
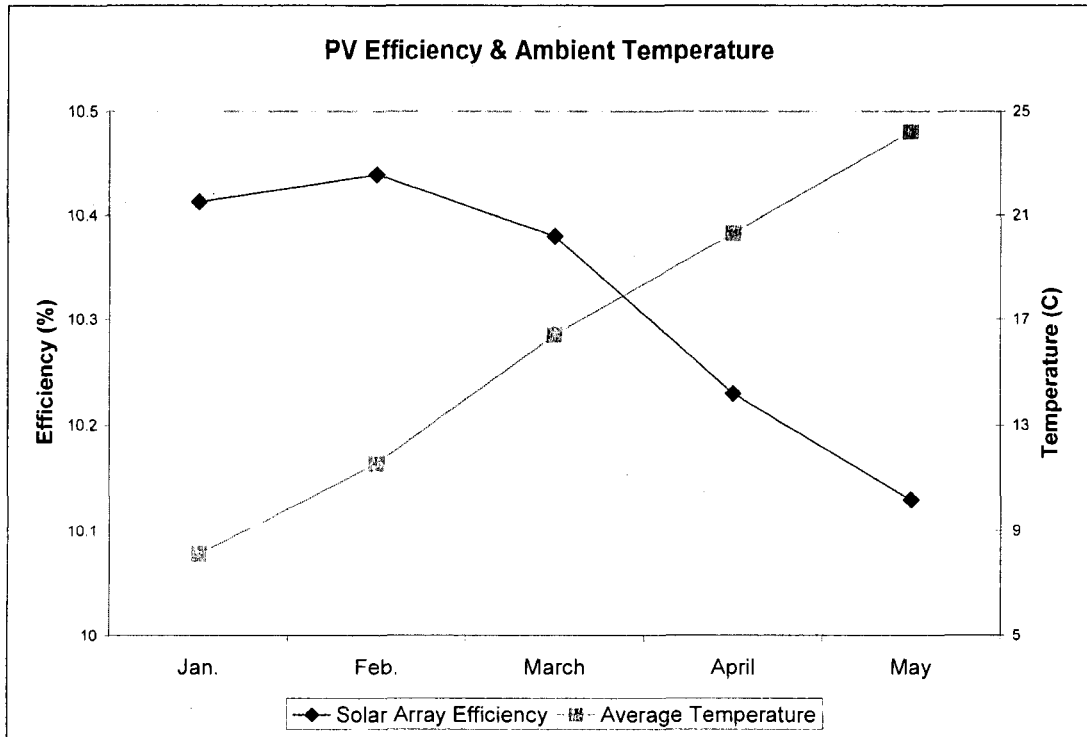
Figure 31. PV efficiency and ambient temperature for Jan.-May 2008.

To show how the HFS will perform under its daily operational demands, hydrogen was dispensed from Unit 2 on June 20, 2008. The amount of hydrogen dispensed was chosen to simulate filling the Ford F-150 pickup truck with enough hydrogen to drive 28.5 miles. The truck will be used as a meter-reading vehicle, and is required to drive approximately 57 miles per day, in two four hour shifts. Therefore, the truck will fill two times each day, and based on an expected fuel efficiency of 16 miles per kilogram of hydrogen [23], approximately 1.78 kg of hydrogen must be dispensed. During the testing, 1.5 kg of hydrogen was dispensed, and the amount of energy required to produce that hydrogen was recorded. Figure 32 shows the power use of the HFS equipment for June 20.
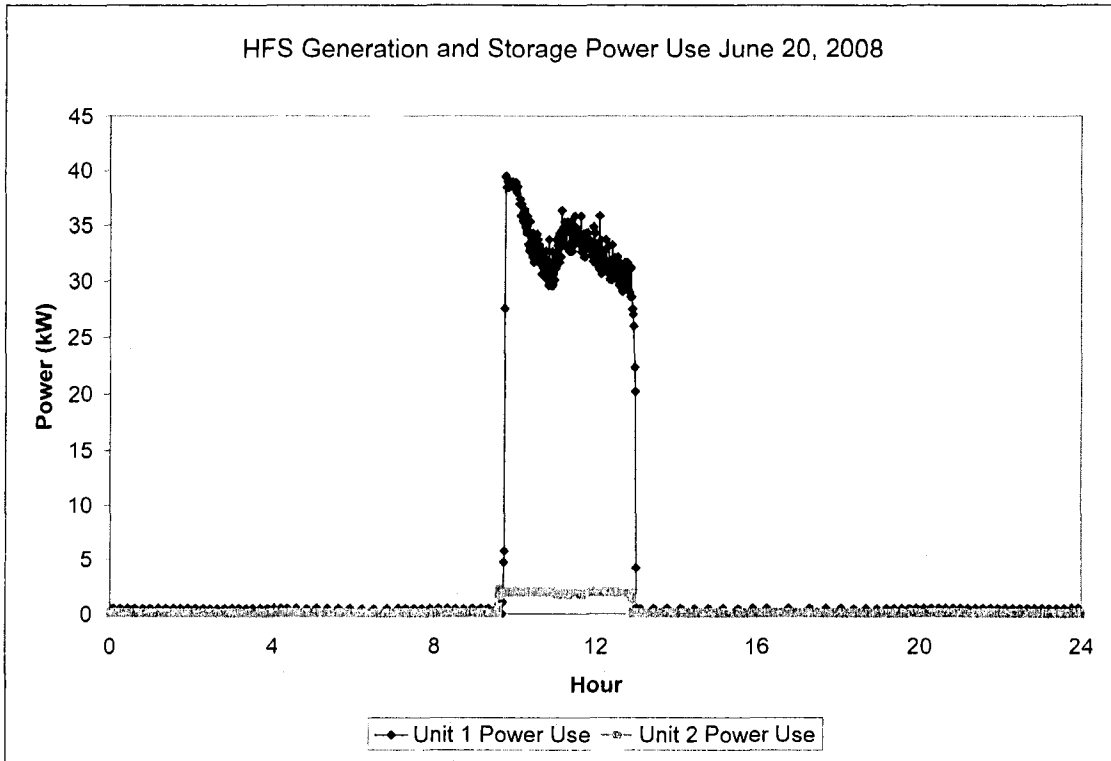
Figure 32. HFS equipment power usage on June 20, 2008.

Power production from the solar PV array for June 20 is shown in Figure 33.
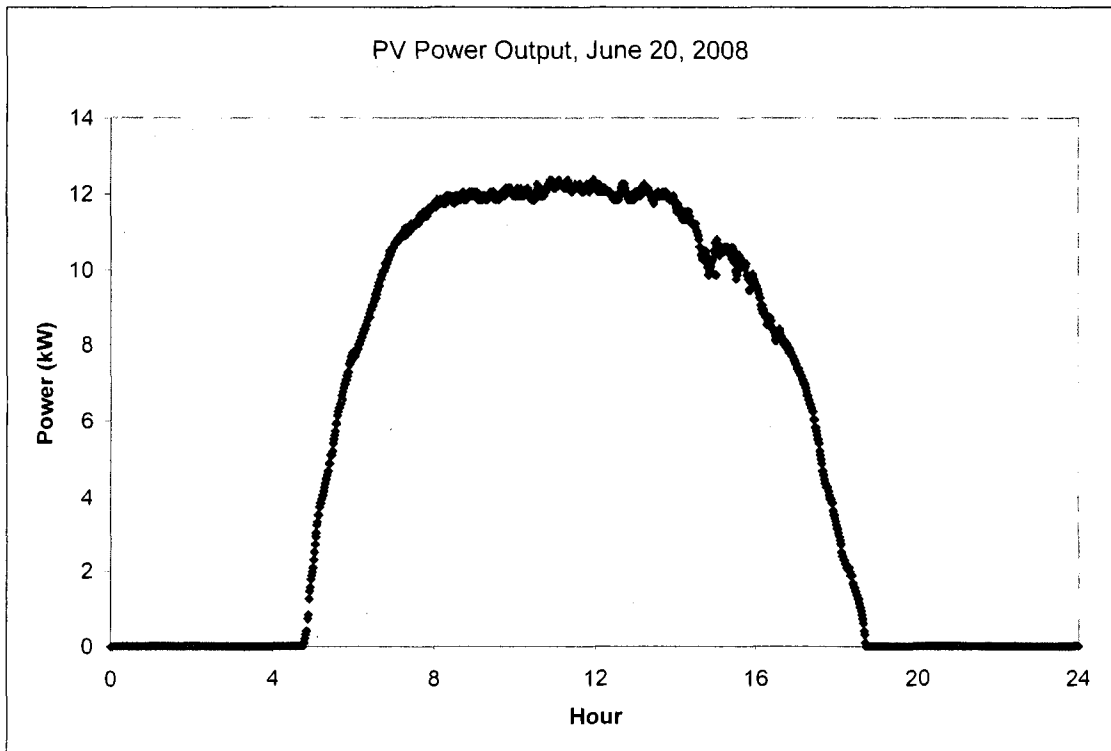
Figure 33. PV array output for June 20, 2008.

41

Finally, the net power flow at the HFS during testing on June 20, 2008 is shown in Figure 34. It is noted that during hydrogen production, the electrolyzer requires much more power than the solar PV array is capable of producing.
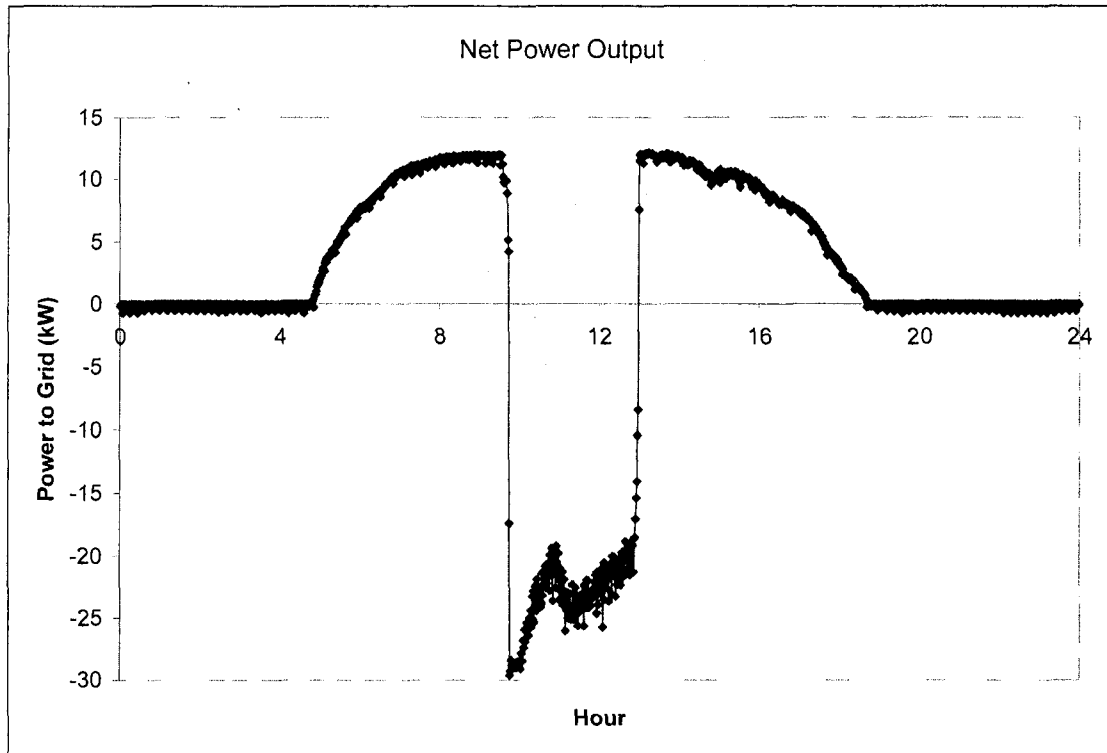
Figure 34. Net power to/from grid during June 20, 2008.

Additionally, it was important to record how quickly the HFS was able to refill its tanks for another fill. This measurement provided a way to determine the amount of use that the station can permit daily. Table 5 shows a summary of how the HFS performed during the simulated fill testing. To produce 1.5 kg of hydrogen, the station required 113.83 kWh. This resulted in a requirement of 75.87 kWh/kg of hydrogen, and an HFS production efficiency of 51.9%.

Table 5.	Phase III June 20, 2008 Test Results
Mass Generated by HFS	1.50 kg
Energy Consumed	113.83 kWh
PV Energy Produced	46.09 kWh
Production Power Requirement	75.87 kWh/kg
HFS Hydrogen Production Efficiency	51.91 %

Figure 35 shows the hydrogen levels in the buffer tank and the dispensing unit based on the maximum mass each is capable of holding, after the 1.50 kg of hydrogen was used. The buffer tank remained over 94% full for the duration of the test, due to the fact that the hydrogen generation rate was similar to the flow rate of the compressor used to refill the tanks in Unit 1. After the fill, the dispenser level dropped to 76%, and required 176 minutes or 2.93 hours to completely refill the tanks on Unit 2 and the buffer tank.
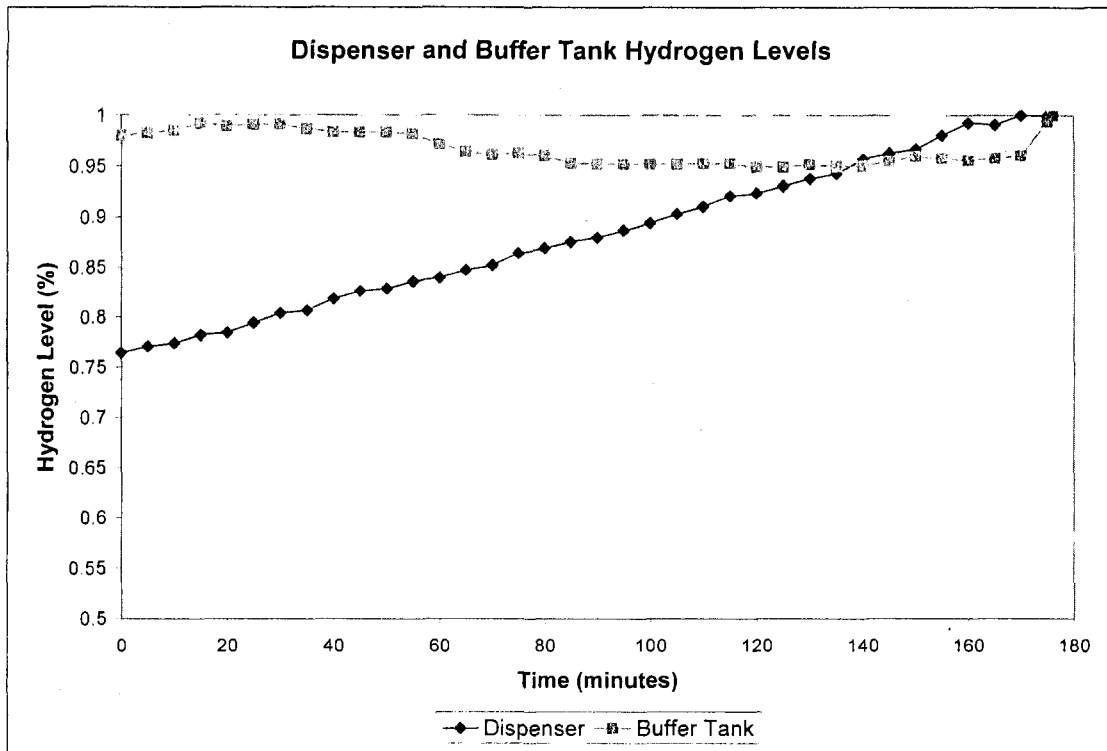
Figure 35. Dispenser and buffer tank hydrogen levels during production, June 20, 2008.

CHAPTER 5

PHASE III HFS COMPUTER MODEL

A computer model has been created to simulate the energy production and use at the

station, as well as how vehicle usage affects the energy and hydrogen balance at the

station. This model is a modification of a previous model used in the original design of

the HFS [15]. The model's inputs include the hourly ambient temperature, wind speed,

and solar irradiance values for a typical year in the Las Vegas region, based on the TMY2

data base [24]. This data is used to predict the performance of the solar PV array at the

HFS. Additionally, manufacturers' and measured data describing the power use of the

HFS equipment were used as inputs for the model. The other model input was an

estimated amount of hydrogen use by the vehicles at the station. The model's outputs

included the total power produced by the solar PV array, the amount of hydrogen

required by the vehicles, and the amount of energy required by the HFS equipment to

refill the tanks at the station. Also, the hydrogen level inside the storage tanks was

modeled, in order to determine the amount of time the station required to return to full

capacity after a vehicle was filled. The model is used to simulate each minute of the

typical year, in order to accurately describe the transient behavior of the HFS equipment.

Since the TMY2 data is given as average hourly data, linear interpolation was used to

estimate the values of the desired parameters for each minute.

Solar PV Array Performance Modeling

To determine the power produced by the solar PV array, the model must calculate the amount of radiation from the sun that is available to the surface of the array. First, the values for global horizontal radiation (I) and diffuse horizontal radiation (I_d) were used from the TMY2 database and interpolated for each minute of the day. Next, a model developed by Braun and Mitchell was used to calculate the surface slope (β) of the single-axis tracking units, since the surface slope varies throughout the day [25]:

$$\beta = \beta_o' + 180\,\sigma_\beta \tag{2}$$

Where:

$$\beta_o' = \tan^{-1}\left(\frac{\tan\beta'}{\cos(\gamma - \gamma')}\right) \tag{3}$$

and

$$\sigma_\beta = \begin{cases} 0 \; if \beta_o' \geq 0 \\ 1 \, otherwise \end{cases} \tag{4}$$

Here, the slope of the tracking axis is β'=30, and γ and γ' are the surface azimuth angle and azimuth angle of the tracking axis (γ'=0 since tracker is facing south) respectively.

A model developed by Perez [26] was then used determine the total amount of diffuse radiation available on the surface of the solar PV array, using data from the TMY2 database and the calculated surface slope of the tracker. The total diffuse radiation is calculated by:

$$I_{d,T} = I_d\left[F_1\frac{a}{b} + F_2\sin\beta + (1 - F_1)(\frac{1 + \cos\beta}{2})\right] \tag{5}$$

Where F_1 and F_2 are brightness coefficients calculated from a number of statistically derived coefficients for a range of sky conditions, as shown in [26], and:

$$\frac{a}{b} = R_b = \frac{\max(0, \cos \vartheta)}{\max(\cos 85, \cos \vartheta_z)} \quad (6)$$

Here, θ is the angle of incidence, the angle between the beam radiation on a surface and the normal of that surface, and θ_z is the zenith angle, the angle of beam radiation on a horizontal surface. R_b is the ratio of beam radiation on a tilted surface to that on a horizontal surface, and is used by the method from Duffie and Beckman, to calculate the total amount of radiation on the tilted surface [27]:

$$I_T = I_b R_b + I\rho_g \left(\frac{1 - \cos \beta}{2}\right) + I_{d,T} \quad (7)$$

where $\rho_g = 0.4$ is the reflectance of the ground and:

$$I_b = I - I_d \quad (8)$$

Once the total available solar radiation is calculated, it is necessary to accurately predict the performance of the specific type of solar PV panel installed at the HFS. This can be done by using the single diode model, which is described by the equivalent circuit given in Figure 36.
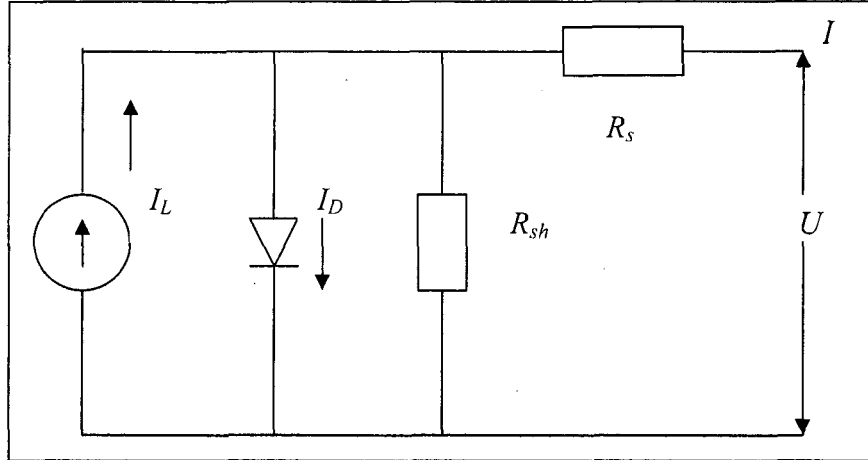
Figure 36. Single diode model of a solar PV panel [27].

The single diode model uses data provided by the panel manufacturer such as short circuit current (I_{sc}=5.4 A), open circuit voltage (U_{oc}=44.4 V), current at maximum power point (I_{mp}=4.95 A), voltage at maximum power point (U_{mp}=35.4 V), as well as temperature coefficients, μ_{Isc}=0.001895 and μ_{Uoc}=-0.093773, to model the PV performance by calculating reference parameters for the panel. This data is given for the standard conditions of the panel, 1000 W/m^2 and panel temperature 25°C.

To determine the power output of each panel, the current-voltage characteristics of the panel are calculated as a function of incident solar irradiation and cell temperature using equation 9 [27]:

$$I_{pv} = I_L - I_O \left[\exp \left[\frac{U_{pv} + I_{pv} R_s}{a} \right] - 1 \right] - \frac{U_{pv} + I_{pv} R_s}{R_{sh}} \quad (9)$$

Where light current (I_L), diode reverse saturation current (I_O), series resistance (R_s), shunt resistant (R_{sh}) and the modified ideality factor (a) are the five parameters that are needed to solve equation 9. Based on the given manufacturer's data, five equations are

47

solved simultaneously with the method shown in [27], to obtain the values of these parameters using the given current-voltage points at the short circuit current, open circuit voltage, and maximum power point. These reference parameters are further used to calculate the operating parameters the PV panel at any the conditions at each minute of the typical meteorological year. The modified ideality factor is found with equation 10:

$$a = \frac{nkT_{pv}N_{PV}}{q} \tag{10}$$

with ideality factor n, Boltzmann's constant k (1.381×10^{-23} J/K), electronic charge q (1.609×10^{-19} A-s), number of solar panel cells in series N_{PV}, and cell temperature T_{pv}.

As shown by equation 10, performance of the solar PV array is dependent on the cell temperature, which itself is a function of solar irradiation, ambient temperature, wind speed, and other factors. Using meteorological data from the TMY2 database, the panel temperature can be calculated as an explicit function of incident solar irradiation, ambient temperature and wind speed using equations 11 and 12 [28].

$$T_{pv} = T_{m,pv} + \frac{I_T}{I_{NOCT}}\Delta T_{pv} \tag{11}$$

where $I_{NOCT} = 1000 W/m^2$ is the instantaneous solar irradiation at standard rated conditions, and $T_{m,pv}$ is the back surface temperature of the panel, given by:

$$T_{m,pv} = T_a + I_T \cdot e^{\left(a_c + b_c V_w\right)} \tag{12}$$

where T_a is the ambient temperature, a_c and b_c are empirical constants, and V_w is the instantaneous wind speed.

Hydrogen demand of the pickup truck is the parameter that drives the HFS performance model. The amount of hydrogen required by the truck was calculated based on its expected daily distance traveled and expected performance, which was assumed to be 16 miles per kilogram of hydrogen, based on previous research [23]. Assuming the daily travel of 57 miles and, that the truck would be fuelled two times a day at 8 AM and noon for two 4 hour shifts, the amount of hydrogen required per fill was found to be 1.78 kg.

Hydrogen generation, storage and utilization were modeled to predict the performance of the HFS. The gas levels of the storage tanks and flow rates were considered on a mass flow basis to eliminate the effects of pressure changes throughout the system. The model was carried out for each month of a typical year, to predict the performance of the equipment and ensure that the HFS met the hydrogen demand of the vehicle.

At the beginning of each month both the buffer tank and dispenser storage tanks were assumed to be 100% full. The compressor started only if the hydrogen level inside the dispenser fell below 90% and the hydrogen level inside the buffer tank was greater than 40 %. From experimental data, the compressor has been shown to use 2 kW during operation, and that it draws hydrogen from the buffer tank at 0.045 kg per minute. The electrolyzer started producing hydrogen when the hydrogen level inside the buffer tank fell below 93 %.

Based on manufacturer's and observed experimental data, the performance of the electrolyzer was be estimated by a fairly simple conversion for this analysis. It has been

49

shown that the FuelGen 12 electrolyzer uses approximately 39 kW during hydrogen production, which agrees with published data regarding electrolyzer operation [29]. The production rate at this level of power use is 0.009 kg of hydrogen per minute. During electrolyzer operation the coolant used to maintain the PEM cell stack temperature begins to heat up, and triggers the auxiliary chiller to operate. From experimentally collected data at the station, the chiller draws between 1 and 4 kW during operation. Additionally, the chiller tends to run more in the summer months when ambient temperatures are high. Therefore, the chiller was modeled to run simultaneously with the electrolyzer, at a fraction of its rated power, depending on the average temperature of the month. Figure 37 shows a flow chart for the simulation.
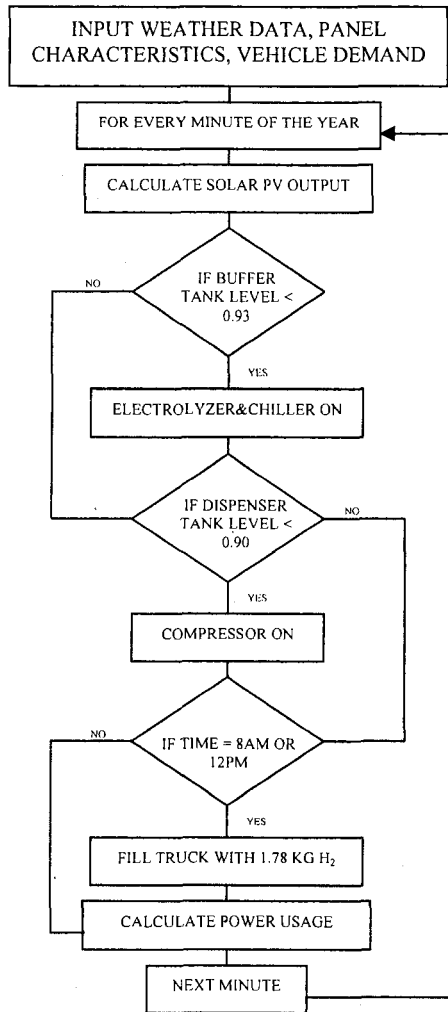
Figure 37. Flow diagram for HFS simulation program.

Combined, the solar PV array and HFS calculations fully describe the energy use and hydrogen production at the station for each minute of one typical year. Based on current station characteristics, the monthly contribution of solar energy to the total energy use of the station is shown in Figure 38. The energy contribution of the solar PV array ranges between a low of 25.7% in December and a maximum of 40.8% in May.
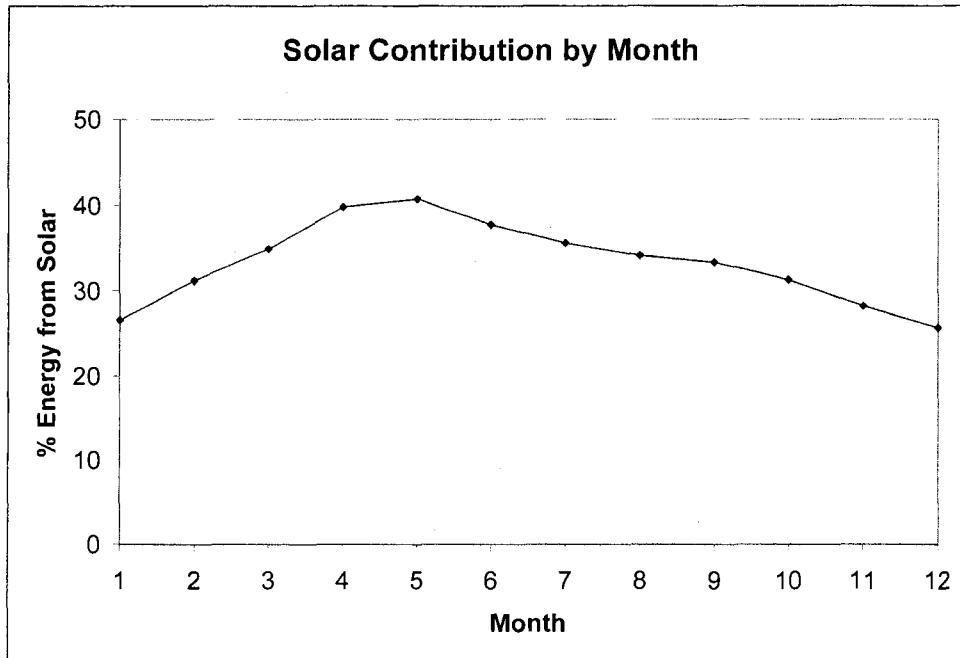
Figure 38. Monthly solar PV contribution to HFS power consumption.

Based on the hydrogen demand described above, the station is required to produce a total of 1292.1 kg of hydrogen in one year, of which almost 431 kg is produced by solar energy. The efficiency of the hydrogen generation and storage processes was again calculated by dividing the energy required to produce and compress the hydrogen by the energy contained in that amount hydrogen, according to its HHV. Therefore, the efficiency of the station was dependent on the assumptions about energy usage from each piece of equipment, and in this case it was calculated to be 49.3%. Based on the expected fuel efficiency of the truck, the 14 kW AC solar PV array is capable of supporting 19 of the 57 miles per day required by the truck. Table 2 shows overall performance data from the model. In order to fully supply the power required to produce the amount of hydrogen necessary to drive the truck 57 miles per day, the solar PV array would need to

be increased to 50.4 kW. This could be accomplished with 8 additional single axis tracking units.

Table 6: Estimated Average Yearly Station Performance

Hydrogen Production	1292.1 kg
Solar Energy Production	34.39 MWh
Solar Contribution to Hydrogen Production	33.34 %
Hydrogen Produced from Solar Energy	430.87 kg
Hydrogen Generation/Compression Efficiency (HHV)	49.3 %

The hydrogen level in the dispenser is shown for a sample day in Figure 39. The minimum level of hydrogen in the unit 2 dispenser is 63% of its capacity. Additionally, it took 2.83 hours for the dispenser to return to 90% of its capacity. This indicates that the station is capable of dispensing more hydrogen during each fill, which could potentially increase the range of the truck. If the truck was filled until the dispenser level reached 50%, its range would increase by over 80% to over 50 miles per fill (formerly 28.5 miles per fill). However, any extra mileage driven by the truck would decrease the percentage of solar energy's input to the total energy required by the HFS.
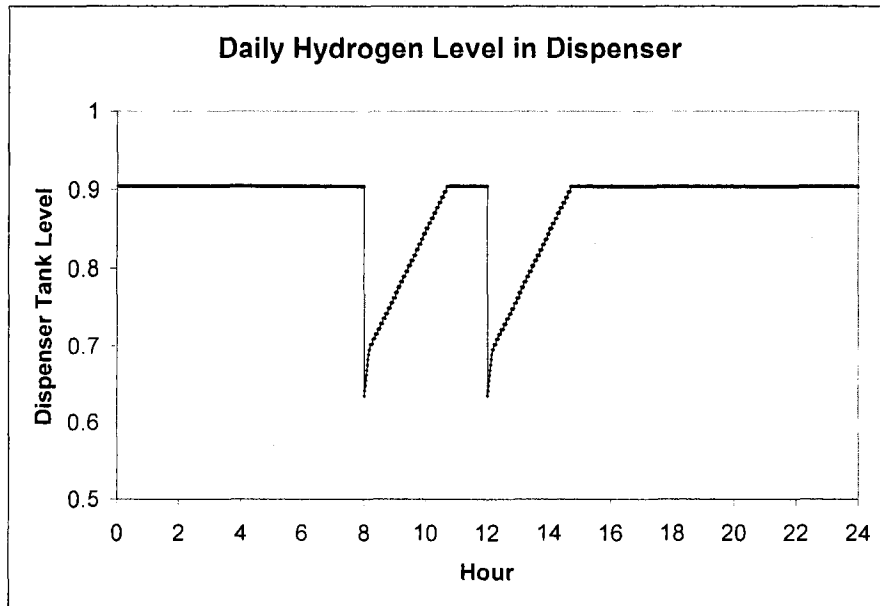
Figure 39. Daily hydrogen level in dispenser as predicted by HFS model.

Hydrogen level in the buffer tank is shown for a sample day in Figure 40. It is shown that the buffer tank level cycles up and down due to the hydrogen input from the electrolyzer and output into the dispenser. Again, it is noted that the minimum level of the tank only drops to 45%, indicating that more hydrogen could be drawn during each fill. It is also important to note that this result was quite different than the result obtained during the experimental testing of the Phase III HFS from June 20, 2008. Therefore, the model needs to be updated to more accurately depict the flow of hydrogen into and out of the buffer tank.
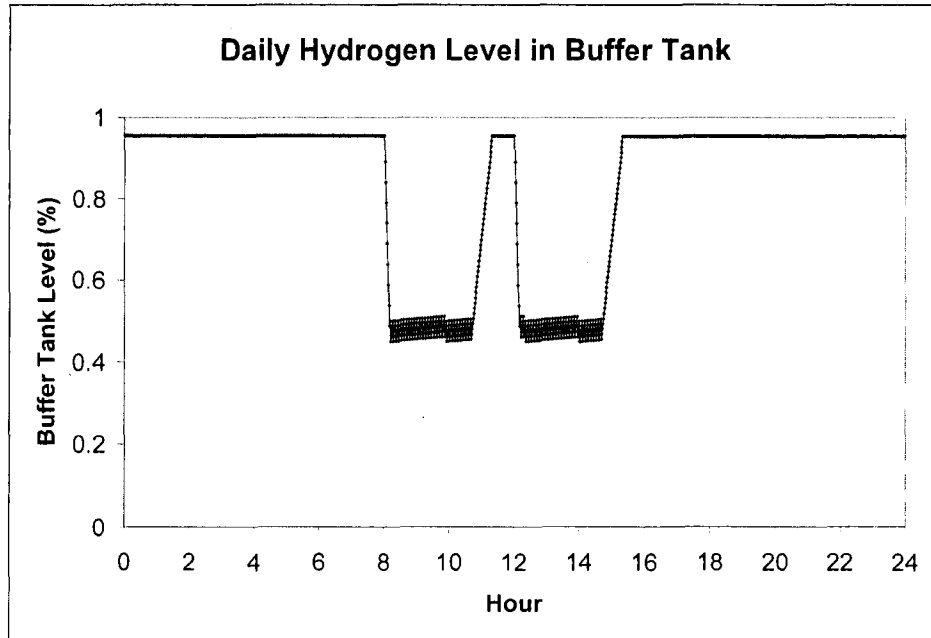
Figure 40. Daily hydrogen level in buffer tank as predicted by HFS model.

Typical daily net power curves vary based on the solar energy production at the station. Two different sample days are shown in Figure 41, for opposite times (summer (a) and winter (b)) of the year. It is noted that although the hydrogen deficiency at 8 AM and noon results in the same drop in net power to the grid, the amount of solar power drastically increases for the month of June.
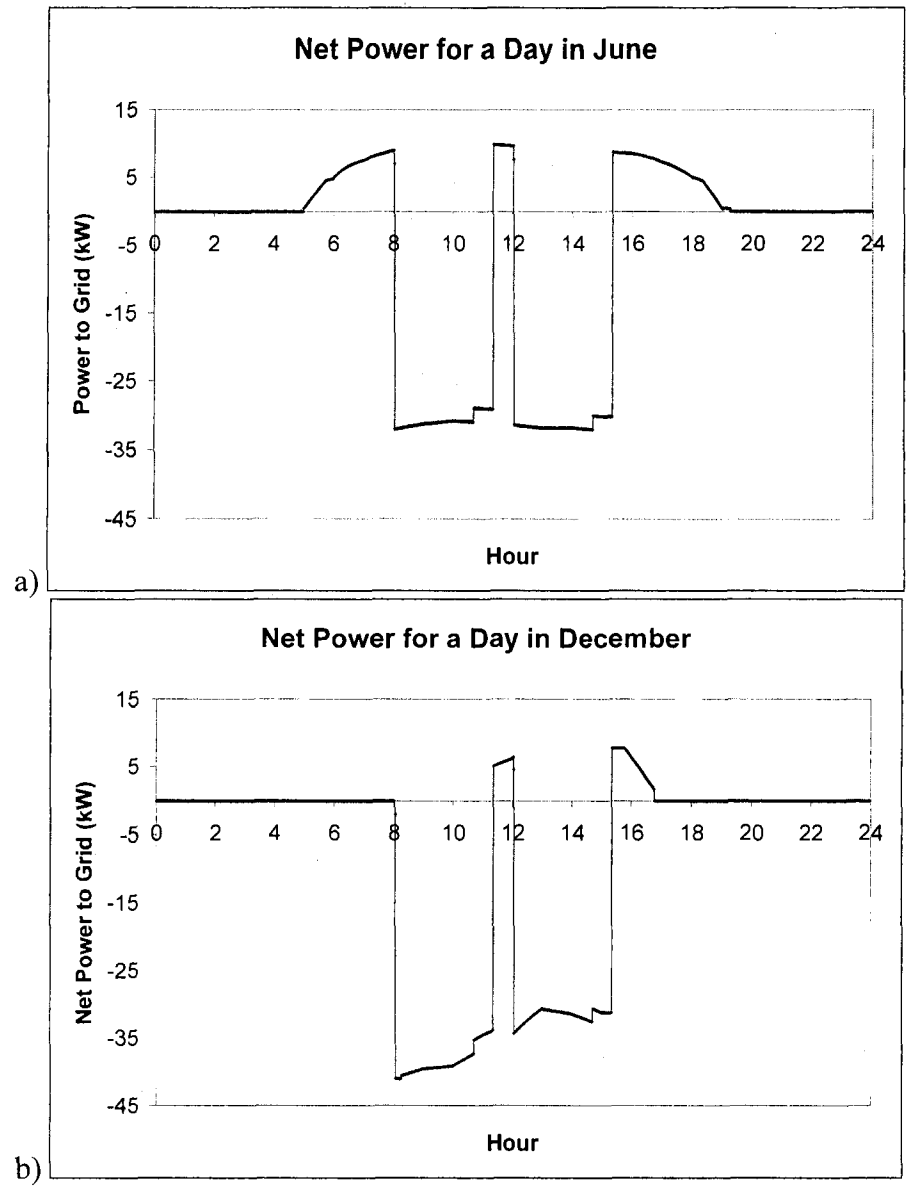
Figure 41. Daily net power to grid in June (a) and December (b).

The daily net power plot for June compares well to what was observed during the June 20, 2008 testing results, as shown in Figure 42. The net power drops to approximately -30 kW (meaning electricity is being used from the grid) during hydrogen production, and slightly increases over the almost 3 hours of hydrogen production.
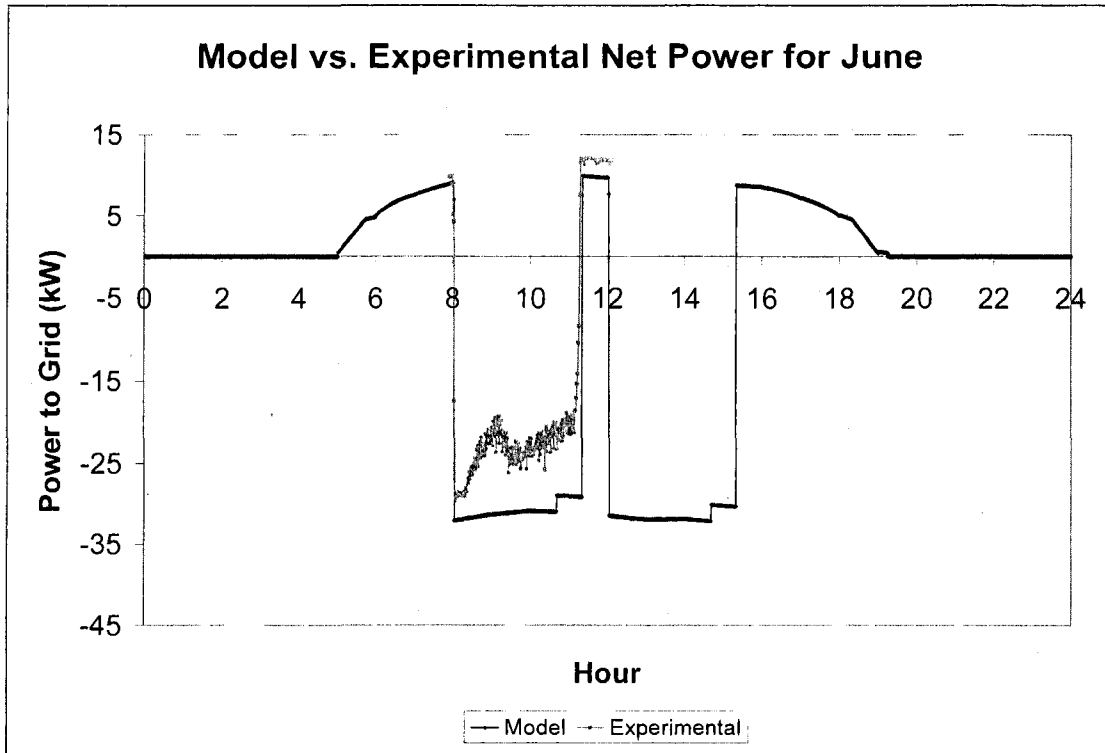
Figure 42. Modeled and experimental net power plots for a day in June.

CHAPTER 6

SUMMARY AND CONCLUSIONS

A hydrogen filling station has been demonstrated, and has operated successfully with several different types of equipment over one and a half years in Las Vegas. The HFS is unique, in that a portion of the energy used to create hydrogen is powered by a solar PV array, and that the electrolysis process used to produce hydrogen is performed by a PEM electrolyzer. This thesis has described the data acquisition system responsible for the collection of data and monitoring of the station's performance. Data have been collected to show the amount of energy produced and consumed at the station, and the resulting efficiency of using solar PV generated electricity to produce hydrogen.

A computer model was created to simulate the operation of the HFS, and was found to agree well with experimental data. The model predicted that, in its current configuration, 33.34 % of the hydrogen produced at the HFS was obtained from solar energy, which amounted to 430.87 kg of hydrogen for a typical year of operation. Because this station was originally configured to power a PEM electrolyzer that produced 2 kg of hydrogen per day while using 8.5-9 kW during operation, the extra energy required to operate the upgraded equipment now at the station exceeds the capacity of the solar PV array currently installed at the HFS. It was found that 8 additional trackers were

required to supply enough energy to produce the 1292.1 kg of hydrogen required by the vehicle for one year.

The computer model was found to agree well with experimental data collected at the Phase III HFS. The net power plots for June compared in Figure 42 show that the net power plot resulting from the model matched well with what was observed during the experimental fill testing on June 20, 2008. Also, the amount of time required to refill the tanks in the dispensing unit after one fill was 2.83 hours for the model case, and 2.93 hours for the experimental testing.

The model does require several modifications to accurately describe the behavior of all HFS systems. First, the rates of hydrogen flow into and out of the buffer tank must be adjusted. Next, more power use observations should be incorporated into the model to better describe how the chiller operates in different climactic conditions. Then, different filling scenarios should be compared to optimize the station's usefulness. Finally, the model should be applied to other regions, to demonstrate how an HFS would perform in different areas.

APPENDIX

Phase II HFS Data Acquisition System Wiring Diagrams

Hydrogen Filling Station Data Acquisition Wiring Schedule

CR10X Datalogger

AM16/32 (COM GND), AM16/32 (PWR GND)	G		G	
	G		G	CS500 (HMP 50) (Clear)
Enclosure Thermocouple	1H		4H	CS500 (HMP 50) (Black)
Enclosure Thermocouple	1L		4L	CS500 (HMP 50) (White)
	AG		AG	CS500 (HMP 50) (Blue)
	2H		5H	03001 Wind (Red) (V)
	2L		5L	
	AG		AG	03001 Wind White (V)
AM16/32 (COM:ODD H)	3H		6H	LI 200X (Red)
AM16/32 (COM:ODD L)	3L		6L	LI 200X (Black)
	AG		AG	LI 200X (White)
03001 Wind (Black) (V)	E1		E3	
	AG		AG	
	E2		G	03001 Wind Clear (V)
	G		G	LI 200X (Clear/Green)
03001 Wind (Black) (A)	P1		5V	
03001 Wind (White) (A), 03001 Wind (Clear) (A)	G		5V	
	P2		G	
	G		SW 12V	
	C8		SW 12V	
	C7		G	
	C6			
AM16/32 (RES)	C5			
AM16/32 (CLK)	C4			
SDM-SW8A (C3)	C3			
SDM-SW8A (C2)	C2			
SDM-SW8A (C1 IN)	C1			
SDM-SW8A (GND)	G			
SDM-SW8A (12V)	12V			
AM16/32 (12V), CS500 (HMP 50) (Brown)	12V			

(Type J Thermocouples)

	16L			32L	
	16H	SET8	SET16	32H	
	15L			31L	
	15H			31H	
	SHIELD			SHIELD	
	14L			30L	
	14H	SET7	SET15	30H	
	13L			29L	
	13H			29H	
	12L			28L	
	12H	SET6	SET14	28H	
	11L			27L	
	11H			27H	
	SHIELD			SHIELD	
	10L			26L	
	10H	SET5	SET13	26H	
	9L			25L	
	9H			25H	
	8L			24L	
	8H	SET4	SET12	24H	
	7L			23L	
	7H			23H	
	SHIELD			SHIELD	
	6L			22L	
	6H	SET3	SET11	22H	
	5L			21L	
	5H			21H	
	COM:EVEN L		COM:ODD L		CR10X (3L)
	SHIELD		SHIELD		CR10X (G)
	COM:EVEN H		COM:ODD H		CR10X (3H)
	4L			20L	
	4H	SET2	SET10	20H	
	3L			19L	
	3H			19H	
	SHIELD			SHIELD	
PV_Temp 2 (red)	2L			18L	
PV_Temp 2 (white)	2H	SET1	SET9	18H	
PV_Temp 1 (red)	1L			17L	
PV_Temp 1 (white)	1H			17H	
				12V	CR10X (12V)
				GND	CR10X (G)
				RES	CR10X (C5)
				CLK	CR10X (C4)

AM16/32 Mode = "2 x 32"

SDM/SMA Pulse Input Module

Power Supply (12V)	**12V**	
CR10X (G)	**GND**	
CR10X (C3)	**C3**	
CR10X (C2)	**C2**	
CR10X (C1)	**C1 IN**	
SDM-SW8A (C1 IN)	**C1 OUT**	
Wattnode Mains IN -	**GND**	
	5V	**SPST Mode**
Wattnode Mains IN +	**IN 1**	
Wattnode Mains OUT -	**GND**	
	5V	**SPST Mode**
Wattnode Mains OUT +	**IN 2**	
Wattnode Dispenser - (Unit 2)	**GND**	
	5V	**SPST Mode**
Wattnode Dispenser + (Unit 2)	**IN 3**	
Wattnode PV OUT -	**GND**	
	5V	**SPST Mode**
Wattnode PV OUT +	**IN 4**	
Wattnode Unit 4 Compressor -	**GND**	
	5V	**SPST Mode**
Wattnode Unit 4 Compressor +	**IN 5**	
Wattnode Unit 4 Chiller -	**GND**	
	5V	**SPST Mode**
Wattnode Unit 4 Chiller +	**IN 6**	
Wattnode Unit 1 LP Electrolyzer -	**GND**	
	5V	**SPST Mode**
Wattnode Unit 1 LP Electrolyzer +	**IN 7**	
Wattnode Unit 3 HP Electrolyzer -	**GND**	
	5V	**SPST Mode**
Wattnode Unit 3 HP Electrolyzer +	**IN 8**	

Phase III HFS Wiring Diagrams

CR10X Datalogger

AM16/32 (COM GND), AM16/32 (PWR GND)	G	G	
	G	G	CS500 (HMP 50) (Clear)
Enclosure Thermocouple	1H	4H	CS500 (HMP 50) (Black)
Enclosure Thermocouple	1L	4L	CS500 (HMP 50) (White)
	AG	AG	CS500 (HMP 50) (Blue)
	2H	5H	03001 Wind (Red) (V)
	2L	5L	
	AG	AG	03001 Wind White (V)
AM16/32 (COM:ODD H)	3H	6H	LI 200X (Red)
AM16/32 (COM:ODD L)	3L	6L	LI 200X (Black)
	AG	AG	LI 200X (White)
03001 Wind (Black) (V)	E1	E3	
	AG	AG	
	E2	G	03001 Wind Clear (V)
	G	G	LI 200X (Clear/Green)
03001 Wind (Black) (A)	P1	5V	
03001 Wind (White) (A), 03001 Wind (Clear) (A)	G	5V	
Flowmeter (pulse input)	P2	G	
Flowmeter (pulse gnd)	G	SW 12V	
	C8	SW 12V	
	C7	G	
	C6		
AM16/32 (RES)	C5		
AM16/32 (CLK)	C4		
SDM-SW8A (C3)	C3		
SDM-SW8A (C2)	C2		
SDM-SW8A (C1 IN)	C1		
SDM-SW8A (GND)	G		
SDM-SW8A (12V)	12V		
AM16/32 (12V), CS500 (HMP 50) (Brown)	12V		

SDM-SW8A
Pulse Input Module

Power Supply (12V)	**12V**	
CR10X (G)	**GND**	
CR10X (C3)	**C3**	
CR10X (C2)	**C2**	
CR10X (C1)	**C1 IN**	
SDM-SW8A (C1 IN)	**C1 OUT**	
Wattnode Mains IN -	**GND**	
	5V	**SPST Mode**
Wattnode Mains IN +	**IN 1**	
Wattnode Mains OUT -	**GND**	
	5V	**SPST Mode**
Wattnode Mains OUT +	**IN 2**	
Wattnode Dispenser - (Unit 2)	**GND**	
	5V	**SPST Mode**
Wattnode Dispenser + (Unit 2)	**IN 3**	
Wattnode PV OUT -	**GND**	
	5V	**SPST Mode**
Wattnode PV OUT +	**IN 4**	
Wattnode Unit 1 Electrolyzer 480V -	**GND**	
	5V	**SPST Mode**
Wattnode Unit 1 Electrolyzer 480V +	**IN 5**	
Wattnode Unit 1A Chiller -	**GND**	
	5V	**SPST Mode**
Wattnode Unit 1A Chiller +	**IN 6**	
Wattnode Unit 1 Electrolyzer 240V -	**GND**	
	5V	**SPST Mode**
Wattnode Unit 1 Electrolyzer 240V +	**IN 7**	
Wattnode Spare -	**GND**	
	5V	**SPST Mode**
Wattnode Spare +	**IN 8**	

*Table 1 Program
 01: 60.0000   Execution Interval (seconds)

1: Batt Voltage (P10)
 1: 1   Loc [Batt_Volt]

2: If time is (P92)
 1: 0   Minutes (Seconds --) into a
 2: 1440   Interval (same units as above)
 3: 30   Then Do

3: Signature (P19)
 1: 2   Loc [Prog_Sig]

4: End (P95)

5: Internal Temperature (P17) ;Reference temperature
 1: 3   Loc [RefTemp   ]

6: Thermocouple Temp (DIFF) (P14) ;Enclosure Temperature
 1: 1   Reps
 2: 1   2.5 mV Slow Range
 3: 1   DIFF Channel
 4: 4   Type J (Iron-Constantan)
 5: 3   Ref Temp (Deg. C) Loc [RefTemp   ]
 6: 4   Loc [EncTemp   ]
 7: 1   Multiplier
 8: 0   Offset

7: Volt (Diff) (P2)
 1: 1   Reps
 2: 14   250 mV Fast Range
 3: 2   DIFF Channel
 4: 5   Loc [OPEN   ]
 5: 1.0   Multiplier
 6: 0.0   Offset

8: Do (P86) ;Activates the Multiplexer
 1: 44   Set Port 4 High

; Start Reading Thermocouples, PV1 and PV2

9: Beginning of Loop (P87)
 1: 0000   Delay
 2: 32   Loop Count

10: Do (P86)
 1: 75   Pulse Port 5

11: Excitation with Delay (P22)
 1: 1   Ex Channel
 2: 1   Delay W/Ex (0.01 sec units)
 3: 100   Delay After Ex (0.01 sec units)

4: 0   mV Excitation

12: Thermocouple Temp (DIFF) (P14) ;J Type Thermocouple on Multiplexer
1: 1   Reps
2: 1   2.5 mV Slow Range
3: 3   DIFF Channel
4: 4   Type J (Iron-Constantan)
5: 3   RefTemp (Deg. C) Loc [RefTemp   ]
6: 6   -- Loc [PVTemp1_C] ;This input location is indexed (--) with the loop
7: 1   Multiplier
8: 0   Offset

13: End (P95)

14: Do (P86) ;Deactivating the Multiplexer
1: 54   Set Port 4 Low

; Following is the energy metering

15: SDM-SW8A (P102) ;Energy for Mains_in
1: 1   Reps
2: 0   SDM Address
3: 2   Counts function
4: 1   SDM-SW8A Starting Channel
5: 14   Loc [Main1kWh]
6: 0.011542 Multiplier ; WattNodeModel 3Y-480, CT Size 200A, in KWh
7: 0   Offset

16: SDM-SW8A (P102) ;Energy for Mains_Out
1: 1   Reps
2: 00   SDM Address
3: 2   Counts function
4: 2   SDM-SW8A Starting Channel
5: 15   Loc [MainOkWh]
6: .011542 Multiplier ; WattNodeModel 3Y-480, CT Size 200A, in KWh
7: 0.0   Offset

17: SDM-SW8A (P102) ;Energy for Dispenser (new model, same parameters)
1: 1   Reps
2: 0   SDM Address
3: 2   Counts function
4: 3   SDM-SW8A Starting Channel
5: 16   Loc [DispkWh]
6: 0.002885 Multiplier ; WattNodeModel 3Y-480, CT Size 50A, in KWh
7: 0   Offset

18: SDM-SW8A (P102) ;Energy for PV generation
1: 1   Reps
2: 00   SDM Address
3: 2   Counts function
4: 4   SDM-SW8A Starting Channel
5: 17   Loc [PVkWh   ]
6: .001731 Multiplier ; WattNodeModel 3Y-480, CT Size 30A, in KWh
7: 0.0   Offset

19: SDM-SW8A (P102) ;Energy for Unit 1 480 V (formerly Unit4)
1: 1   Reps
2: 0   SDM Address
3: 2   Counts function
4: 5   SDM-SW8A Starting Channel
5: 18   Loc [U1480kWh]
6: .008656 Multiplier ; WattNodeModel 3Y-480, CT Size 150A, in KWh
7: 0   Offset

20: SDM-SW8A (P102) ;Energy for Unit 1A Chiller (formerly unit 4b chiller)
1: 1   Reps
2: 00   SDM Address
3: 2   Counts function
4: 6   SDM-SW8A Starting Channel
5: 19   Loc [U1AkWh   ]
6: .005771 Multiplier ; WattNodeModel 3Y-480, CT Size 100A, in KWh
7: 0.0   Offset

21: SDM-SW8A (P102) ;Energy for Unit 1 240 V (formerly total Unit 1 energy)
1: 1   Reps
2: 0   SDM Address
3: 2   Counts function
4: 7   SDM-SW8A Starting Channel
5: 20   Loc [U1240kWh]
6: .00075 Multiplier ; WattNodeModel 1P-240, CT Size 30A, in KWh
7: 0   Offset

22: SDM-SW8A (P102) ; Spare Wattnode (formerly Energy for Unit3)
1: 1   Reps
2: 00   SDM Address
3: 2   Counts function
4: 8   SDM-SW8A Starting Channel
5: 21   Loc [SparekWh]
6: 0.0025 Multiplier ; WattNodeModel 1P-240, CT Size 100A, in KWh
7: 0.0   Offset

;End of energy metering

23: Volt (SE) (P1) ;Ambient temperature measurement
1: 1   Reps
2: 25   2500 mV 60 Hz Rejection Range
3: 7   SE Channel
4: 8   Loc [AmbT_C   ]
5: 0.1   Multiplier ;Probe Model CS500, Degrees Celsius
6: -40.0 Offset ;Probe Model CS500, Degrees Celsius

24: Volt (SE) (P1) ;Relative Humidity measurement
1: 1   Reps
2: 25   2500 mV 60 Hz Rejection Range
3: 8   SE Channel
4: 9   Loc [RH_PER   ]
5: 0.1   Multiplier ;Probe Model CS500, Percent
6: 0   Offset

25: If (X<=>F) (P89)
1: 9   X Loc [RH_PER   ]
2: 3   >=
3: 100   F
4: 30   Then Do

26: If (X<=>F) (P89)
1: 9   X Loc [RH_PER   ]
2: 4   <
3: 108   F
4: 30   Then Do

27: Z=F x 10^n (P30)
1: 100   F
2: 0   n, Exponent of 10
3: 9   Z Loc [RH_PER   ]

28: End (P95)

29: End (P95)

30: Pulse (P3) ;Wind Speed Measurement
1: 1   Reps
2: 1   Pulse Channel 1
3: 21   Low Level AC, Output Hz
4: 10   Loc [WS_ms   ]
5: 0.75   Multiplier ;Model 03001 Wind, m/s
6: 0.2   Offset ;Model 03001 Wind, m/s

31: If (X<=>F) (P89)
1: 10   X Loc [WS_ms   ]
2: 4   <
3: 0.21   F
4: 30   Then Do

32: Z=F x 10^n (P30)
1: 0   F
2: 0   n, Exponent of 10
3: 10   Z Loc [WS_ms   ]

33: End (P95)

34: Pulse (P3) ;This is hydrogen generation
1: 1   Reps
2: 2   Pulse Channel 2
3: 21   Low Level AC, Output Hz
4: 22   Loc [H2Gen_kg]
5: 0.01667 Multiplier
6: 0.0   Offset

35: Excite-Delay (SE) (P4) ;Wind Direction Measurement
1: 1   Reps
2: 5   2500 mV Slow Range
3: 9   SE Channel
4: 1   Excite all reps w/Exchan 1
5: 2   Delay (0.01 sec units)

6: 2500   mV Excitation
7: 11   Loc [WindDir_D]
8: 0.142   Multiplier ;Model 03001 Wind, CR10X
9: 0   Offset ;Model 03001 Wind, CR10X

36: If (X<=>F) (P89)
1: 11   X Loc [WindDir_D]
2: 3   >=
3: 360   F
4: 30   Then Do

37: Z=F x 10^n (P30)
1: 0   F
2: 0   n, Exponent of 10
3: 11   Z Loc [WindDir_D]

38: End (P95)

39: Volt (Diff) (P2) ;Incident Solar Radiation measurement
1: 1   Reps
2: 22   7.5 mV 60 Hz Rejection Range
3: 6   DIFF Channel
4: 12   Loc [IncRad_W]
5: 1   Multiplier ;Model LI200X pyranometer, no multiplier
6: 0   Offset

40: If (X<=>F) (P89)
1: 12   X Loc [IncRad_W]
2: 4   <
3: 0   F
4: 30   Then Do

41: Z=F x 10^n (P30)
1: 0   F
2: 0   n, Exponent of 10
3: 12   Z Loc [IncRad_W]

42: End (P95)

*43: Z=X*F (P37) ;Convert raw incident radiation to MJ*
1: 12   X Loc [IncRad_W]
*2: 0.012   F ;Model LI200X, MJ/m^2, scan interval(60s)*0.0002*
3: 13   Z Loc [IncRad_MJ]

*44: Z=X*F (P37) ;Convert raw incident radiation to W*
1: 12   X Loc [IncRad_W]
2: 200   F ;Model LI200X, W/m^2
3: 12   Z Loc [IncRad_W]

;This section converts our energy readings to instantaneous power
;and stores it in a new output location, multiply by 60 to get kW from kWh/min

*45: Z=X*F (P37)*
1: 14   X Loc [MainIkWh]
2: 60   F
3: 23   Z Loc [MainIkW]

69

46: Z=X*F (P37)
1: 15   X Loc [MainOkWh]
2: 60   F
3: 24   Z Loc [MainOkW]

47: Z=X*F (P37)
1: 16   X Loc [DispkWh]
2: 60   F
3: 25   Z Loc [DispkW]

48: Z=X*F (P37)
1: 17   X Loc [PVkWh   ]
2: 60   F
3: 26   Z Loc [PVkW   ]

49: Z=X*F (P37)
1: 18   X Loc [U1480kWh]
2: 60   F
3: 27   Z Loc [U1480kW]

50: Z=X*F (P37)
1: 19   X Loc [U1AkWh]
2: 60   F
3: 28   Z Loc [U1AkW   ]

51: Z=X*F (P37)
1: 20   X Loc [U1240kWh]
2: 60   F
3: 29   Z Loc [U1240kW]

52: Z=X*F (P37)
1: 21   X Loc [SparekWh]
2: 60   F
3: 30   Z Loc [SparekW]

;End of energy to power conversions

53: If time is (P92)
1: 0   Minutes (Seconds --) into a
2: 1   Interval (same units as above)
3: 10   Set Output Flag High (Flag 0)

54: Set Active Storage Area (P80)^15853;Now start writing data to output locations
1: 1   Final Storage Area 1
2: 101   Array ID

55: Real Time (P77)^4812
1: 1220   Year,Day,Hour/Minute (midnight = 2400)

56: Sample (P70)^28896
1: 1   Reps
2: 5   Loc [OPEN   ]

57: Average (P71)^19346
1: 1   Reps

2: 6   Loc [PVTemp1_C]

58: Average (P71)^31813
1: 1   Reps
2: 7   Loc [PVTemp2_C]

59: Average (P71)^18495
1: 1   Reps
2: 8   Loc [AmbT_C   ]

60: Sample (P70)^17501
1: 1   Reps
2: 9   Loc [RH_PER   ]

61: Average (P71)^14120
1: 1   Reps
2: 10   Loc [WS_ms   ]

62: Sample (P70)^19815
1: 1   Reps
2: 11   Loc [WindDir_D]

63: Average (P71)^13251
1: 1   Reps
2: 12   Loc [IncRad_W]

64: Resolution (P78) ;Set to high resolution for radiation and energy output
1: 1   High Resolution

65: Totalize (P72)^23582
1: 1   Reps
2: 13   Loc [IncRad_MJ]

66: Totalize (P72)^16263
1: 8   Reps
2: 14   Loc [MainIkWh]

67: Totalize (P72)^24387
1: 1   Reps
2: 22   Loc [H2Gen_kg]

68: Resolution (P78) ;Set back to low resolution
1: 0 .   Low Resolution

69: Sample (P70)^19082
1: 8   Reps
2: 23   Loc [MainIkW]

70: If time is (P92)
1: 0   Minutes (Seconds --) into a
2: 1440   Interval (same units as above)
3: 10   Set Output Flag High (Flag 0)

71: Set Active Storage Area (P80)^1261
1: 1   Final Storage Area 1
2: 102   Array ID

72: Real Time (P77)^30382
1: 1220   Year,Day,Hour/Minute (midnight = 2400)

73: Minimum (P74)^6336
1: 1   Reps
2: 0   Value Only
3: 1   Loc [Batt_Volt]

74: Sample (P70)^14555
1: 1   Reps
2: 2   Loc [Prog_Sig]

*Table 2 Program
01: 10.0000   Execution Interval (seconds)

1: Serial Out (P96)
1: 71   Storage Module

*Table 3 Subroutines

End Program

```
function datatodata

%this program will take the final storage .dat file and
%output for each day the same daily data from the split program such as the
%average/max temperature, wind speed, and power usage numbers....
%reading the comma data from the data logger
datalogger = csvread('Hydrogen Station_final_storage_5.dat',0,0);

day = datalogger(:,3);
lof = length(day);

%here is how to get the correct day to collect and output to the filename

todaynow = now;
yesterday = todaynow -1;
gooday = datestr(yesterday);

%need to get realgoodday as the day of the year 1-365, not between 1-30 or
%31 because the program is running at 5am, the round will be sure to be
%yesterday

yestrnd = round(yesterday);
realgoodday = yestrnd - 733408; % it must actually be the number of the day

mymonthstr = datestr(yesterday,'mmmm');
myyearstr = datestr(yesterday, 'yyyy');
mydaystr = datestr(yesterday, 'dd');
myfilestr = [mymonthstr, myyearstr,'.dat'];

%here going to decrease the value of x in datalogger(x,3) until its value
%is equal to the value of the daytocollect the do until it is not equal

i=lof; %length of file
while datalogger(i,3) ~= realgoodday
    i = i-1;
end

i = i-1; %here have to get rid of the first line which is from array
         %102 in the data file
index = 1;

while datalogger(i,3) == realgoodday
    %output each desired column to its new array here for each day.
    %output array is actually in decending order starting at the end of the
    %day and going until the beginning - doesn't matter for sums and
    %averages.
    desireddatafile(index,1) = datalogger(i,3); %day
    desireddatafile(index,2) = datalogger(i,4); %time
    desireddatafile(index,3) = datalogger(i,8); %temperature
    desireddatafile(index,4) = datalogger(i,10); %wind speed
    desireddatafile(index,5) = datalogger(i,12); %available energy
    desireddatafile(index,6) = datalogger(i,14); %mains in kWh
    desireddatafile(index,7) = datalogger(i,15); %mains out kWh
```

```
    desireddatafile(index,8) = datalogger(i,16); %dispenser kWh
    desireddatafile(index,9) = datalogger(i,26); %pv kW
    desireddatafile(index,10) = datalogger(i,17); %pv kWh
    desireddatafile(index,11) = datalogger(i,18); %Unit 1 480 kWh
    desireddatafile(index,12) = datalogger(i,19); %Unit 1A kWh
    desireddatafile(index,13) = datalogger(i,20); %Unit 1 240 kWh
    desireddatafile(index,14) = datalogger(i,21); %spare kWh
    desireddatafile(index,15) = datalogger(i,22); %hydrogen produced
    i = i-1;
    index = index + 1;
end
%need lenght of the file to get all the data from the one day.

lof2 = length(desireddatafile(:,1));

%this looks at the data for one day to get the values want to output
averagetemp = mean(desireddatafile([1:lof2],3));
maxtemp = max(desireddatafile([1:lof2],3));
averagews = mean(desireddatafile([1:lof2],4));
maxws = max(desireddatafile([1:lof2],4));
totenergyav = sum(desireddatafile([1:lof2],5))/1000.0/60.0 ;
mainincol = desireddatafile(:,6);
mainsin = sum(desireddatafile([1:lof2],6));
mainsout = sum(desireddatafile([1:lof2],7));
dispenser = sum(desireddatafile([1:lof2],8));
pvmax = max(desireddatafile([1:lof2],9));
pvpower = sum(desireddatafile([1:lof2],10));
unit1480 = sum(desireddatafile([1:lof2],11));
unit1a = sum(desireddatafile([1:lof2],12));
unit1240 = sum(desireddatafile([1:lof2],13));
Spare = sum(desireddatafile([1:lof2],14));
H2Gen = sum(desireddatafile([1:lof2],15));

%this makes one row of the data to output for the day

rightnow = now; % this part gets the date
yest = rightnow - 1; %  this way if day you are collecting is first of
mynewvector = datevec(yest); %month, then it won't show 0 as the day
dailydata(1,1) = mynewvector(3); % it will show 30 or 31

dailydata(1,2) = maxtemp;
dailydata(1,3) = averagetemp;
dailydata(1,4) = maxws;
dailydata(1,5) = averagews;
dailydata(1,6) = totenergyav;
dailydata(1,7) = mainsin;
dailydata(1,8) = mainsout;
dailydata(1,9) = dispenser;
dailydata(1,10) = pvmax;
dailydata(1,11) = pvpower;
dailydata(1,12) = unit1480;
dailydata(1,13) = unit1a;
dailydata(1,14) = unit1240;
dailydata(1,15) = Spare;
dailydata(1,16) = dailydata(1,12) + dailydata(1,14);
dailydata(1,17) = H2Gen;
```

```
%%%%%%%%%%%%%%%%%%%%%%%%%%%%%%%%%%%%%%%%%%%%%%%%%%%

Creating the data file and bar chart

%if myfilestr exists, then append the file with the row of data from
%dailydata, if not, then create a new file for the next month
fid=0;
%fopen(['N:\htdocs\wwwhydrogen\data\',myfilestr],'w');
fid = fopen(['N:\htdocs\wwwhydrogen\data\',myfilestr],'r');

if fid == -1
    %create the file here because it doesn't exist
    pleasework = fopen(['N:\htdocs\wwwhydrogen\data\',myfilestr],'w');

fprintf(pleasework,'%s\r','Day,MaxTemp.,Avg.Temp.,MaxWindSpeed,Avg.WindSpeed,TotalAvailEnergy,Ma
insIN,MainsOUT,Dispenser,MaxPVOut,PVOUT,Unit1480,Unit1A,Unit1240,Spare,Unit1Tot');
    %fprintf(pleasework,);
    fprintf(pleasework,'%s\r','of
Month,Deg.C,Deg.C,m/s,m/s,kWh/m^2,kWh,kWh,kWh,kW,kWh,kWh,kWh,kWh,kWh,kg');
    fprintf(pleasework,'%0.0f%s',dailydata(1,1),',');
    %loop to print out the first day's data
    m=2;
    for m = 2:16
        fprintf(pleasework,'%0.2f%s',dailydata(1,m),',');
        m = m+1;
    end
    %get rid of last comma and add a return
    fprintf(pleasework,'%0.3f\r',dailydata(1,m));
%%%%%%%%%%%%%%%%%%%%%%%%%%%%%%%%%%%%%%%%%%%%%%%%%%%%%%%%%%%%%
else if fid >=1
        %if the loop goes here then we are just adding a line of text to an
        %existing file, and hopefully the bar plot will update as well.
        %need to append the file
        pleasework1 = fopen(['N:\htdocs\wwwhydrogen\data\',myfilestr],'a');
        fprintf(pleasework1,'%0.0f%s',dailydata(1,1),',');
        %loop to print out the additional day's data
        m=2;
        for m = 2:16
            fprintf(pleasework1,'%0.2f%s',dailydata(1,m),',');
            m = m+1;
        end
        %get rid of last comma and add a return
        fprintf(pleasework1,'%0.3f\r',dailydata(1,m));
    end
%%%%%%%%%%%%%%%%%%%%%%%%%%%%%%%%%%%%%%%%%%%%%%%%%%%%%%%%%%%%%

end
%reading from the data file to make the bar charts
fclose('all');

data1=csvread(['N:\htdocs\wwwhydrogen\data\',myfilestr],2,0);
day1=data1(:,1);
PowerIn=data1(:,7);
PowerOut=data1(:,8);
NetPower=PowerOut-PowerIn;
s=[PowerIn,PowerOut,NetPower];
```

75

```
%%%%%%%%%%%%%%%%%%%%%%%%%%%%%%%%%%%%%%%%%%%%%%%%%%%%%%%%%
%BARCHART making

BarChart = figure('Position',[150 150 480 360],'PaperPosition',[150 150 4.8 3.6]);
%% Create axes
axes1 = axes('FontSize',8,'Position',[0.1308 0.146 0.7092 0.766],'XGrid','on',...
    'Box','on','Parent',BarChart);
axis(axes1,[0 32 0 134.6]);
xlim(axes1,[0 32]);
set(axes1,'xtick',[0 2 4 6 8 10 12 14 16 18 20 22 24 26 28 30]);
set(axes1,'YLimMode', 'auto');
%need to put the month's name in the title here
title(axes1,[mymonthstr, ' ', myyearstr, ' Net System Power']);
%need add the month's name in the x label date
xlabel(axes1,['Day of ', mymonthstr,' ', myyearstr]);
ylabel(axes1,'Power (kWh)');
hold(axes1,'all');
%% Create bar
bar(s,'group')
%% Create legend
legend1 = legend(...
  axes1,{'Equipment Power Use','PV Power Output','Net Power to Grid'},...
  'FontSize',5,...
  'Position',[0.1233 0.006025 0.7215 0.04167],...
  'Orientation','horizontal');
%now want to add code that saves the file as a picture with the same
%filename as a .png
saveas(BarChart, ['N:\htdocs\wwwhydrogen\data\',mymonthstr, myyearstr, '.png'],'png');
close(BarChart);

END OF PROGRAM
```

Matlab HFS Simulation Code

This program is the simulation of the HFS, it has inputs from the TMY2 weather data and hydrogen equipment performance

```
clear all
close all
clc
tic

% This program gives input for each time step to different components and
% received output

% PV PANELS
% POWER CONDITIONING ( CONVERTER AND INVERTER )
% BUSBAR
% ELECTROLYZER
% COMPRESSOR
% STORAGE TANK
% FUEL CELL
% hydext=0;
hydext=0.0667 + 0.1886;
%---------------size of tank----------------------------
tksiz= 2.4;  % Volume of storage vessel [cu.m]
rated_fc=1000;  % Watts
ncells_fc=24;
%----------------------------------------------------------
arpvp= 4;  % Number of PV-modules in parallel in PV-Array  [-]
arpvs= 24;   % Number of PV-modules in series in PV-Array    [-]
%----------------------------------------------------------
glevnext=0.6; minlev=0.05; maxlev=0.95;

hrelec=0;
hrfc=0;
%***********************************************************************
% subroutine perez calculates solar radiation on tilted surface and ambient
% temperature data
delt=1; % min
parsim(1)=745;   % Tstart [>=1]
parsim(2)=1417;  % Tstop  [<=8759]
parsim(3)=delt;  % delta t(min)
parsim(4)=4;   % tracking type
parsim(5)=0;   % slope: slope of the collector
parsim(6)=0;   % azm: surface azimuth angle due south=0, east -ve, west +ve)
parsim(7)=30;  % betad: slope of tracking axis
parsim(8)=0;   % tazm: tracking axis angle due south=0, east -ve, west +ve)

[n,LT,gt,Tambin, loadsys, wspeed]= perez(parsim);
tt=[1:1:n]';
loadsys=loadsys;
%-----------------------------------------------------------
%-----------------Array parameters--------------------------
parpv(1)= arpvp;    % Number of PV-modules in parallel in PV-Array  [-]
parpv(2)= arpvs;    % Number of PV-modules in series in PV-Array    [-]
%-----------------------------------------------------------
```

```
% Sharp 175 Watt
%-----------------Manufacturer's data--------------------------
parpv(3)= 72;  %    Number of cells in series
parpv(4)= 5.55; % Isc  Short circuit current at reference conditions [Amps]
parpv(5)= 4.95;% Imp    Current at maximum power point ----"------ [Amps]
parpv(6)= 44.4;% Voc    Open circuit voltage --------"--------------[Volts]
parpv(7)= 35.4;% Vmp    Voltage st maximum power point ----"----- [Volts]
parpv(8)= 0.000351*parpv(4);
% uIsc Temp. coefficient of short circuit current[Amps/K]
parpv(9)= -0.093775;% uVoc Temp. coefficient of open circuit voltage [Amps/K]
parpv(10)= 1.3009;   %  Area (Single PV panel)          [m^2]
% Based on material from which pv panels are made
parpv(11)= 1.12;  %     egap
parpv(12)= 153.7;  %    Rsh shunt resistance
% Conditions at noct
parpv(13)= 298;  %   Tanoct   Ambient Temp at noct [K]
parpv(14)= 320;  %   Tnoct   cell temp at noct   [K]
parpv(15)= 1000;  %  gnoct               [W/m2]
% Calculation of cell temperature parameters
parpv(16)= -3.5588; %   a   Constant from PV design pro
parpv(17)= -0.0752;%   b   Constant from PV design pro
parpv(18)= 2;  %      dt  Tc-Tm evaluated at 1000 w/m2


ratedpv= parpv(1)*parpv(2)*parpv(5)*parpv(7);
rati= parpv(5)*parpv(1);
ratv= parpv(7)*parpv(2);


%  ************** endofpv *************
%  ************** Power conditioning (Inverter) ***************
% Parameters
parpc(1)= 1;     % 1=connected to power source/ 2=connected to load
parpc(2)= 1500;    % Nominal power [W] (approx. 20 % less than rated power)
parpc(3)= 5.846e-3;% Idling constant (popn= po/pn)
parpc(4)= 2.06;  % set point voltage [V]
parpc(5)= 138.42; % Internal resistance constant(ripn= ri*pn) [v^2]
parpc(6)= 1;     % Number power conditioner modules connected in parallel
parpc(7)= 0;     % Auxillary power needed to operate power connditioner [W]


% *******************End Power Conditioning**********************


% hydrogen vehicle characteristics
mileage = 16;  %miles/kg
dailydistance = 57; %miles driven per day with two fills
hperday = dailydistance/mileage; % total hydrogen needed per day
hperfill = hperday/2;  % if fill vehicle twice need half daily hydrogen
numtanks = hperfill/2.233133;  %2.233133 kg per tank at 350 bar
% buffer and dispenser tank initial levels
glevbuf=1;
glevdis=1;


% **********input************

inpv(1)=1;
Tnow=75;
nini=1; % for storage tank
Toldfc=70;
```

```
for i=1:n
    dayhour(i)=LT(i)-((ceil(LT(i)/24)-1)*24);
    % Inputs for PV panels
    inpv(2)=i;
    inpv(3)=gt(i);
    inpv(4)= Tambin(i);
    inpv(5)= wspeed(i);

    % outa=pv_perf(inpv,parpv); % PV Calculations
    outa=pvperf5p(inpv,parpv); % PV Calculations
    outpv(:,i)=outa;
    outp=outpv'; % output from Photovoltaic panels

    % Output from pv panels
    pvi=outp(:,1);      % Current [Amps]
    pvv=outp(:,2);      % Voltage [Volts]
    pvp=outp(:,3);      % Power [Watts]
    pveta=outp(:,4);    % Efficiency
    pvT=outp(:,5);      % Temperature of PV-Cell (and PV Array) [K]
    pvisc=outp(:,6);    % Short circuit current [Amps]
    pvvoc=outp(:,7);    % Open circuit voltage [Volts]

%   Inverter

    pwcv=208; % Voltage for inverter
    pwcp(i)=0.92*pvp(i); % At rated conditions (pv output 16.8 kw after inverter 14 kw)
    pwci=pwcp(i)/pwcv;

%   Transformer

    pwcv=480; % Voltage for inverter
    pwct(i)=0.92*pwcp(i); % At rated conditions (pv output 16.8 kw after inverter 14 kw)
    pwci=pwct(i)/pwcv;

%   Equipment Power usage (2 units of electrolyzer, Chiller, heater)

    % *********************** AC mini grid ***********************************
% Parameters
    parbb(1)= 480;      % Voltage on mini grid
    % Inputs
    inpbb(1)= pwct(i);  % Power from photovoltaics (PV) system  [W]
    inpbb(2)= loadsys(i);

% Note
% (0-off, 1-on) Electrolyzer operating switch
% (0-off, 1-on) Compressor

cfrac=1;
    oplev=0.9; % Operating level of dispenser tank

    if glevbuf >= 0.95    % Buffer Storage tank is full
```

79

```
pelec(i,1)=0;   % all power goes to grid
hyprod(i,1)=0; % kg/hour of hydrogen

if glevdis >= oplev
    cctrl=0;   % compressor off
    pcomp(i,1)=0;   % all power goes to grid
else
    cctrl=1;   % compressor on
    pcomp(i,1)=2000*cfrac/(delt/60);   % compressor on
    %check above statement placing
end
%pgrid(i)=pwct(i)-pelec(i)-pcomp(i);   % +ve  goes to the grid
else           % Buffer Storage tank is empty
    pelec(i,1)=39000;  % pgridm=39 kW
    hyprod(i,1)=0.5392/(60/delt);  % kg/hour of hydrogen into buffertank
    btcap=0.702;  % Kg of hydrogen
    %%%%%%%%%%%%%%%%%%%%%%%%%%%%%%%%%%%%%%%%%%%%%%

    if hyprod(i,1) > btcap*(1-glevbuf)
        hyprod(i,1) = (1-glevbuf)*btcap/(60/delt);
        pelec(i,1)=39000*(1-glevbuf);
    end
    %%%%%%%%%%%%%%%%%%%%%%%%%%%%%%%%%%%%%%%%%%%%%%%
    if glevdis >= oplev
        cctrl=0;   % compressor off
        pcomp(i,1)=0;
    else
        cctrl=1;   % compressor on
        pcomp(i,1)=2000*cfrac;
    end
end
% *********** Buffer tank **********************************
    btcap=0.702;  % Kg of hydrogen
    if glevbuf >= 0.5 & cctrl==1
        mcompin(i,1)= 2.67*cfrac/(60/delt);    % mass flow rate out of tank for compressor [kg/hr]

    if mcompin(i)>btcap*glevbuf
        mcompin(i,1) = glevbuf*btcap/(60/delt);
        pcomp(i,1) = 2000*glevbuf;
    end
    else
        mcompin(i,1)= 0 ;   % Volumetric flow rate out of tank for dispenser [Nm^3/hr]
    end
    glevbuf= glevbuf + (hyprod(i)/btcap)-(mcompin(i)/btcap);
    glevelb(i,1)=glevbuf;

% ******* Dispenser storage tank *****************
    dtcap=6.6;  % (kg) of hydrogen in dispenser tank
    if dayhour(i) == 8 | dayhour(i) == 12 % time is 8 am and 12 pm fill the tanks according to shift times
        if glevdis > 0.6
            hydisp(i)= hperfill;  % kg of hydrogen used by vehicles
        else
            hydisp(i)=0;  % no dispensing
        end
    else
        hydisp(i)=0;  % no dispensing
```

```
end
if cctrl==1 % compressor is on
    glevdis= glevdis + (mcompin(i)/dtcap)-(hydisp(i)/dtcap);
else
    glevdis= glevdis -(hydisp(i)/dtcap);
end
gleveld(i)=glevdis;
% ***********************End Dispenser *******************
% calculate power usage
pgrid(i)=pwct(i)-pelec(i)-pcomp(i);  % +ve  goes to the grid
toc
i
end


subplot(331);plot(LT, pgrid)
grid on
legend(' Power from PV Panels ')
title('')
xlabel('Time (Months)'),ylabel('Power W')
% xlim([0 8760]); set(gca,'XTick', mytick)
% set(gca,'XTickLabel',{'1','2','3','4','5','6','7','8','9','10','11','12'})
subplot(332);plot(LT, glevelb)
grid on
legend(' buffer tank level ')
title('')
xlabel('Time (Months)'),ylabel('0-1')
subplot(333);plot(LT, gleveld)
grid on
legend(' dispenser tank level ')
title('')
xlabel('Time (Months)'),ylabel('0-1')
subplot(334);plot(LT, hyprod)
grid on
legend(' hydrogen production ')
title('')
xlabel('Time (Months)'),ylabel('kg')
```

BIBLIOGRAPHY

[1] U.S. Department of Energy, Energy Information Administration, Annual Energy Outlook 2005, (February 2005), 7.

[2] Oak Ridge National Laboratory, Transportation Energy Data Book: Edition 24, (December 2004), "Table 1.13 World Petroleum Production, 1073-2003," 1-4.

[3] Environmental Protection Agency , "Greenhouse Emissions from the U.S. Transportation Sector 1990-2003," EPA 420 R 06 003, March 2006

[4] U.S. Department of Energy, "Solar and Wind Technologies for Hydrogen Production," Report to Congress, ESECS EE-3060, 2005

[5] Nowotny, J., Sorrell, C.C., Sheppard, L.R., Bak, T., "Solar-Hydrogen: Environmentally Safe Fuel for the Future." International Journal of Hydrogen Energy 30 (2005): pp. 521-544

[6] Wang, M., "Fuel Choices for Fuel-Cell Vehicles: Well to Wheels Energy and Emission Impacts." Journal of Power Sources 112 (2002): pp. 307-321.

[7] Turner, J.A., "Sustainable Hydrogen Production." Science 305 (2004): pp. 972-974.

[8] Ivy, J., Levene, J.I., "An Analysis of Hydrogen Production from Renewable Electricity Sources," Solar Energy, 2007, 81, pp. 773-780

[9] Conibeer, G.J., and Richards, B.S., "A Comparison of PV/Electrolyser and Photoelectrolytic Technologies." International Journal of Hydrogen Energy, 2006, doi: 10.1016/j.ijhydene.2006.09.012.

[10] Barbir, F., "PEM Electrolysis for Production of Hydrogen from Renewable Energy Sources," Solar Energy, 2005, 78, pp.661-669.

[11] Vanhanen, J.P., Kauranen, P.S., Lund, P.D., Manninen, L.M., "Simulation of Solar Hydrogen Energy Systems." Solar Energy, 1994, 53, pp. 267-278.

[12] Lehman, P.A., Chamberlin, C.E., "Design of a Photovoltaic-Hydrogen-Fuel Cell Energy System." International Journal of Hydrogen Energy, 1991, 16, pp. 349-352

[13] Bilgen, E., 2004, "Domestic Hydrogen Production Using Renewable Energy," <u>Solar Energy</u>, 77, pp. 47-55.

[14] Mason, J.E., Zweibel, K., "Baseline Model of a Centralized PV Electrolytic Hydrogen System." <u>International Journal of Hydrogen Energy</u>, 2007, doi: 10.1016/j.ijhydene.2006.12.019.

[15] Deshmukh, S.S., Baghzouz, Y., Boehm, R.F., 2006, "Design of Grid Connected-PV System for a Hydrogen Refueling Station," Proc of Int. Solar Energy Conference, Denver, CO, ISEC2006-99151.

[16] Lehman, P.A., Chamberlin, C.E., Pauletto, G., Rocheleau, M.A., "Operating Experience with a Photovoltaic-Hydrogen Energy System," <u>International Journal of Hydrogen Energy</u>, 1997, 22, pp. 465-470

[17] Vidueira, J.M., Contreras, A., Veziroglu, T.N., "PV Autonomous Installation to Produce Hydrogen via Electrolysis, and its use in FC Buses," <u>International Journal of Hydrogen Energy</u>, 2003, 28, pp. 927-937.

[18] Chaparro, A.M, Soler, J., Escudero, M.J., de Ceballos, E.M.L., Wittstadt, U., Daza, L., "Data Results and Operation Experience with a Solar Hydrogen System." <u>Journal of Power Sources</u>, 2005, 144, pp. 165-169.

[19] Kai, T., Uemura, Y., Takanashi, H. Tsutsui, T., Takahashi, T., Matsumoto, Y., Fujie, K., Suzuki, M., "A Demonstration Project of the Hydrogen Station Located on Yakushima Island – Operation and Analysis of the Station." <u>International Journal of Hydrogen Energy</u>, 2007, doi: 10.1016/j.ijhydene.2007.02.015.

[20] Fifield, R., Gardner, J., Boehm, R.F., "Conversion and Performance Analysis of a Small Utility Vehicle Operating on Hydrogen Fuel," Proc. of Energy Sustainability 2007, 2007, Long Beach, CA, ES2007-36106

[21] Gardner, J., "Conversion and Performance Evaluation of a Hydrogen Powered Ford F-250 Pickup Truck," M.S. Thesis, University of Nevada, Las Vegas, Las Vegas, NV, 2007.

[22] Nishioka, K., Hatayama, T., Uraoka, Y., Fuyuki, T., Hagihara, R., Watanabe, M., "Field-test Analysis of PV System Output Characteristics Focusing on Module Temperature." <u>Solar Energy Materials & Solar Cells</u>, 2003, 75, pp. 665-671.

[23] Brayer, R., Karner, D., Francfort, J., 2006, "U.S. Department of Energy FreedomCAR & Vehicle Technologies Program -- Hydrogen and Hydrogen/Natural Gas Station and Vehicle Operations – 2006 Summary Report," INL/EXT-06-11689.

[24] National Solar Radiation Data Base, http://rredc.nrel.gov/solar/old_data/nsrdb/tmy2/, as of June 20, 2008.

[25] Braun, J.E., and Mitchell, J. C., "Solar Geometry for Fixed and Tracking Surfaces," Solar Energy, 1983, 31, pp. 439-444.

[26] Perez, R., Ineichen, P., Seals, R., Michalsky, J., Stewart, R., "Modeling Daylight Availability and Irradiance Components from Direct and Global Irradiance." Solar Energy, 1990, 44, pp. 271-289.

[27] Duffie, J.A., Beckman, W.A., Solar Engineering of Thermal Processes. 3rd ed. New York: John Wiley and Sons, Inc.; 2006.

[28] King, D.L., Boyson, W.E., Krotochvil, J.A., "Photovoltaic Array Performance Model." SAND2004-3535; Aug. 2004.

[29] Ivy, J., "Summary of Electrolytic Hydrogen Production," NREL Milestone Completion Report, NREL/MP-60-36734, 2004.

VITA

Graduate College
University of Nevada, Las Vegas

Mark R. Campbell

Home Address:
   3145 E. Flamingo Rd., Unit 1040
   Las Vegas, Nevada 89121

Degrees:
   Bachelor of Science, Mechanical Engineering, 2004
   University of Pittsburgh

Publications:
   Campbell, M., Hurt, R., Sadineni, S. B., Boehm, R. F., "A Solar Powered Hydrogen Generation and Filling Station." American Solar Energy Society Conference Proceedings (2008).

   Campbell, M., Deshmukh, S., Boehm, R. F., Hurt, R., "Modeling Solar Impacts on Hydrogen Production from Electrolysis." American Society of Mechanical Engineers Energy Sustainability 2008 Conference Proceedings.

Thesis Title: Monitoring and Modeling the Performance of a Solar Powered Hydrogen Filling Station.

Thesis Examination Committee:
   Chairperson, Dr. Robert Boehm
   Committee Member, Dr. Yitung Chen.
   Committee Member, Dr. Woosoon Yim
   Graduate College Representative, Dr. Yahia Baghzouz